



Ramírez-Torres, A., Di Stefano, S., Grillo, A., Rodríguez-Ramos, R., Merodio, J. and Penta, R. (2018) An asymptotic homogenization approach to the microstructural evolution of heterogeneous media. *International Journal of Non-Linear Mechanics*, 106, pp. 245-257. (doi: [10.1016/j.ijnonlinmec.2018.06.012](https://doi.org/10.1016/j.ijnonlinmec.2018.06.012))

There may be differences between this version and the published version. You are advised to consult the publisher's version if you wish to cite from it.

<http://eprints.gla.ac.uk/213054/>

Deposited on: 31 March 2020

Enlighten – Research publications by members of the University of Glasgow  
<http://eprints.gla.ac.uk>

1 An Asymptotic Homogenization Approach to the  
2 Microstructural Evolution of Heterogeneous Media

3 Ariel Ramírez-Torres<sup>a</sup>, Salvatore Di Stefano<sup>a</sup>, Alfio Grillo<sup>a</sup>,  
4 Reinaldo Rodríguez-Ramos<sup>b</sup>, José Merodio<sup>c</sup>, Raimondo Penta<sup>d,\*</sup>

5 <sup>a</sup>*Dipartimento di Scienze Matematiche “G. L. Lagrange”,*  
6 *Politecnico di Torino, Torino, 10129, Italy*

7 <sup>b</sup>*Departamento de Matemáticas, Facultad de Matemática y Computación,*  
8 *Universidad de La Habana, La Habana, CP 10400, Cuba*

9 <sup>c</sup>*Departamento de Mecánica de los Medios Continuos y T. Estructuras,*  
10 *E.T.S. de Caminos, Canales y Puertos,*  
11 *Universidad Politécnica de Madrid, Madrid, CP 28040, Spain*

12 <sup>d</sup>*School of Mathematics and Statistics, Mathematics and Statistics Building,*  
13 *University of Glasgow, University Place, Glasgow G12 8QQ, UK*

---

14 **Abstract**

In the present work, we apply the asymptotic homogenization technique to the equations describing the dynamics of a heterogeneous material with evolving micro-structure, thereby obtaining a set of upscaled, effective equations. We consider the case in which the heterogeneous body comprises two hyper-elastic materials and we assume that the evolution of their micro-structure occurs through the development of plastic-like distortions, the latter ones being accounted for by means of the Bilby-Kröner-Lee (BKL) decomposition. The asymptotic homogenization approach is applied simultaneously to the linear momentum balance law of the body and to the evolution law for the plastic-like distortions. Such evolution law models a stress-driven production of inelastic distortions, and stems from phenomenological observations done on cellular aggregates. The whole study is also framed within the limit of small elastic distortions, and provide a robust framework that can be readily generalized to growth and remodeling of nonlinear composites. **Finally, we complete our theoretical model by performing numerical simulations.**

15 *Keywords:* Asymptotic homogenization, heterogeneous media, remodeling,  
16 BKL decomposition, two-scale plasticity, nonlinear composites

---

<sup>☆</sup>Manuscript submitted to the Special Issue “Multi-scale nonlinear continuum mechanical coupled field modelling and applications”

\*Corresponding author

*Email address:* [raimondo.penta@glasgow.ac.uk](mailto:raimondo.penta@glasgow.ac.uk) (Raimondo Penta)

*Preprint submitted to International Journal of Nonlinear Mechanics*

*June 29, 2018*

17 **1. Introduction**

18 The study of material growth, remodeling and aging is of great impor-  
19 tance in Biomechanics, specially when the tissue, in which these processes  
20 occur, features a very complex structure, with different scales of observation  
21 and various constituents.

22 In the literature, the study of heterogeneous materials follows several  
23 approaches. In this work we focus on the multi-scale asymptotic homoge-  
24 nization technique [4, 5, 8, 14, 77], which exploits the information available  
25 at the smallest scale characterizing the considered medium or phenomenon to  
26 obtain an effective description of the medium or phenomenon itself valid at  
27 its largest scale. This is achieved by expanding in asymptotic series the equa-  
28 tions constituting the mathematical model formulated at the lowest scale. As  
29 a result, the coefficients of the effective governing equations encode the infor-  
30 mation on the other hierarchical levels, as they are to be computed solving  
31 microstructural problems at the smaller scales. The multi-scales asymptotic  
32 homogenization approach has been successfully applied to investigate var-  
33 ious physical systems due to its potentiality in decreasing the complexity  
34 of the problem at hand. Biomechanical applications of asymptotic homoge-  
35 nization may be found mainly in nanomedicine [81], biomaterials modeling,  
36 such as the bone [58], tissue engineering [24], poroelasticity [63], and active  
37 elastomers [64]. Most of the literature concerning applications of the asymp-  
38 totic homogenization technique focuses on linearized governing equations, as  
39 in this case it is possible to obtain, under a number of simplifying assump-  
40 tions, a full decoupling between scales, which leads to a dramatic reduction  
41 in the computational complexity, as also noted for example in [64]. In fact,  
42 homogenization in nonlinear mechanics is usually tackled via average field  
43 approaches based on representative volume elements or Eshelby-based tech-  
44 niques (see, e.g. [41] for a comparison between the latter and asymptotic  
45 homogenization), as done for example in [11]. These homogenization ap-  
46 proaches are typically well-suited when seeking for suitable bounds for the  
47 coefficients of the model, such as the elastic moduli, while asymptotic ho-  
48 mogenization can provide a precise characterization of the coefficients under  
49 appropriate regularity assumptions (namely, *local periodicity*).

50 However, to the best of our knowledge and understanding, there exists  
51 only a few examples, e.g. [15, 68, 74, 75], dealing with the asymptotic ho-  
52 mogenization in the case of media undergoing large deformations. In [68],  
53 the static microstructural effects of periodic hyperelastic composites at finite

54 strain are investigated. In [74], the interactions between large deforming solid  
55 and fluid media at the microscopic level are described by using the two-scale  
56 homogenization technique and the updated Lagrangian formulation. In [15],  
57 the effective equations describing the flow, elastic deformation and transport  
58 in an active poroelastic medium were obtained. Therein, the authors consid-  
59 ered the spatial homogenization of a coupled transport and fluid-structure  
60 interaction model, incorporating details of the microscopic system and ad-  
61 mitting finite growth and deformation at the pore scale. Some works can be  
62 also found dealing with homogenization in the case of elastic perfectly plastic  
63 constituents [79, 83].

64 Here we embrace the asymptotic homogenization approach and consider  
65 a heterogeneous body composed of two hyperelastic solid constituents sub-  
66 jected to the evolution of their internal structure. We refer to this phe-  
67 nomenon as to material remodeling and we interpret it with the production  
68 of plastic-like distortions. The wording “material remodeling” is used as a  
69 synonym of “evolution of the internal structure” of a tissue, and is intended in  
70 the sense of [16], who states that “*biological systems can adapt their structure*  
71 *[...] to accommodate a changed mechanical load environment*”. In this case,  
72 always in the terminology of [16] and [80], one speaks of *epigenetic* adap-  
73 tation (or material remodeling). In the framework of the manuscript, such  
74 adaptation is assumed to occur through plastic-like distortions that represent  
75 processes like the redistribution of the adhesion bonds among the tissue cells.

76 It is worth to recall in which sense the concept of “plastic distortions”,  
77 conceived in the context of the Theory of Plasticity (cf. e.g. [50, 55]),  
78 and originally referred to non-living materials such as metals or soils, can  
79 be imported to describe the structural evolution of biological tissues. To  
80 this end, it is important to emphasize that the wording “plastic distortions”  
81 is understood as the result of a complex of transformations that conducts  
82 to the reorganization of the internal structure of a material, and that —  
83 as anticipated in the Introduction— such reorganization is referred to as  
84 “remodeling” in the biomechanical context.

85 The ways in which the structural transformations may take place in a  
86 given material depend on the structural properties of the material itself. For  
87 this reason, the plasticity in metals is markedly different from that occurring  
88 in amorphous materials. In the case of metals, indeed, for which the internal  
89 structure is granular and characterized by the arrangement of the atomic lat-  
90 tice within each grain, plastic distortions are the *macroscopic* manifestation  
91 of the formation and evolution of lattice defects. As reported in [55], such

92 defects can be due, for example, to edge dislocations, wedge disclinations,  
93 missing atoms at some lattice sites, or to the presence of atoms in the lat-  
94 tice interstices. To describe how the defects evolve, thereby giving rise to the  
95 plastic distortions, one should compare the real lattice at the current instant  
96 of time with an ideal lattice, and decompose the overall deformation (i.e.,  
97 shape change *and* structural transformation) into an elastic and an inelastic  
98 contribution [55]. The elastic contribution describes the part of deformation  
99 that is recoverable by completely relaxing mechanical stress, whereas the in-  
100 elastic contribution represents the structural variation, which, in general, is  
101 of irreversible nature.

102 Clearly, metals have structural features markedly different from those of  
103 living matter. Still, some of the fundamental mechanisms that trigger the  
104 reorganization of their internal structure can be adapted to describe the  
105 remodeling of biological tissues.

106 For instance, in the case of bones, plastic-like phenomena are due to the  
107 formation of microcracks that, in turn, favors the gliding of the material  
108 along the direction of the opening of the cracks [17]. Lastly, as anticipated  
109 above, in the case of biological tissues such as cellular aggregates, the phe-  
110 nomenon analogous to the generation of dislocations is the rearrangement of  
111 the adhesion bonds among the cells or the reorganization of the extracellular  
112 matrix due to the reorientation of the collagen fibers or their deposition and  
113 resorption, as is the case for blood vessels [48]. Also in all these situations,  
114 the comparison of the real configuration of the tissue with an “ideal” one,  
115 taken as reference, permits the separation of the overall deformation into an  
116 elastic part and a structure-related, “plastic-like” part.

117 Here, taking inspiration from the theory of finite Elastoplasticity [55, 78,  
118 34], we describe the plastic-like distortions by invoking the Bilby-Kröner-Lee  
119 (BKL) decomposition of the deformation gradient tensor, and rephrasing it in  
120 a scale-dependent fashion. We remark that, at each of the medium’s charac-  
121 teristic scales, a tensor of plastic distortions is introduced, which accounts for  
122 the fact that the structural variations of the medium cannot be expressed, in  
123 general, in terms of compatible deformations. Our study is conducted within  
124 a purely mechanical framework and under the assumption of negligible iner-  
125 tial forces. These hypotheses imply that the model equations reduce to a set  
126 comprising a scale-dependent, quasi-static law of balance of linear momen-  
127 tum and an evolution law for the tensor of plastic-like distortions. The latter  
128 one is assumed to obey a phenomenological flow rule driven by stress.

129 The manuscript is organized as follows. In Section 2, we introduce the

130 fundamental notions related to the separation of scales, kinematics, and the  
 131 Bilby-Kröner-Lee decomposition for the heterogeneous material. Therein,  
 132 the kinematics of the considered medium is discussed, which has to account  
 133 for the different length-scales characterizing the heterogeneities and results  
 134 into the definition of a scale-dependent deformation gradient tensor. In Sec-  
 135 tion 3, the problem to be solved is formulated, and in Section 4, the two-  
 136 scales asymptotic homogenization technique is applied to obtain the local  
 137 and the homogenized sub-problems. In Section 5, we prescribe a constitutive  
 138 equation for the response of the material, and independently, an evolution  
 139 equation for the tensor of plastic-like distortions. In that respect, the local  
 140 and homogenized problems derived in Section 4 are formulated by consid-  
 141 ering the De Saint-Venant strain energy density and we demonstrate the  
 142 relationship between our new model and the classical ones. In Section 6 we  
 143 outline a computational scheme to solve the resulting up-scaled model [and](#)  
 144 [in Section 7, we address the numerical results of our simulations.](#) Finally,  
 145 some concluding remarks on the ongoing work, along with suggestions for  
 146 future research, are summarized in Section 8. We highlight the novelty of  
 147 our approach, and we explain how it may contribute to the understanding of  
 148 the mechanics of heterogeneous media with evolving micro-structure.

## 149 2. Theoretical background

### 150 2.1. Separation of scales

151 The homogenization of a highly heterogeneous medium is only possible  
 152 when the characteristic length of the the local structure ( $\ell_0$ ) and the char-  
 153 acteristic length of the material, or of the phenomenon, of interest ( $L_0$ ) are  
 154 well separated. This condition of separation of scales can be expressed as

$$\varepsilon_0 := \frac{\ell_0}{L_0} \ll 1. \quad (1)$$

155 There may exist more than two coexisting scales and, if they are well sepa-  
 156 rated from each other, a homogenization approach is possible. In this case,  
 157 we then move from the smallest scale to the largest one by homogenization  
 158 [1, 8, 51, 82, 69].

159 Condition (1) is taken as a base assumption for all homogenization pro-  
 160 cesses. The two characteristic length scales  $\ell_0$  and  $L_0$  introduce two dimen-  
 161 sionless spatial variables in reference configuration,  $\tilde{Y} = X/\ell_0$  and  $\tilde{X} =$   
 162  $X/L_0$ , where  $X$  is said to be the *physical spatial variable*, whereas  $\tilde{Y}$  and

163  $\tilde{X}$  represent the microscopic and the macroscopic non-dimensional spatial  
 164 variables, respectively. By using (1),  $\tilde{Y}$  and  $\tilde{X}$  can be related through the  
 165 expression

$$\tilde{Y} = \varepsilon_0^{-1} \tilde{X}. \quad (2)$$

166 Given a field  $\Phi$  defined over the region of interest of the heterogeneous  
 167 medium, the separation of scales allows to rephrase the space dependence of  
 168  $\Phi$  as  $\Phi(X) = \check{\Phi}(\tilde{X}(X), \tilde{Y}(X))$ , and the spatial derivative of  $\Phi$  takes thus the  
 169 form

$$\text{Grad}_X \Phi = L_0^{-1} (\text{Grad}_{\tilde{X}} \check{\Phi} + \varepsilon_0^{-1} \text{Grad}_{\tilde{Y}} \check{\Phi}). \quad (3)$$

170 By following this approach, all equations should be written in non-dimensional  
 171 form. In the literature, the switch to the auxiliary variables  $\tilde{X}$  and  $\tilde{Y}$  is often  
 172 omitted. However, as shown for example in [4], both paths are equivalent pro-  
 173 vided that the dimensional formulation of the problem consistently accounts  
 174 for any asymptotic behavior of the involved fields and parameters (see, e.g.,  
 175 [62] and the discussion therein concerning problems where such a behavior is  
 176 actually deduced via a non-dimensional analysis). By exploiting this result,  
 177 in what follows our analysis is carried out directly in a system of physical  
 178 variables  $X$  and  $Y$ . Moreover, by adopting the approach usually followed in  
 179 asymptotic multiscale analysis, we assume that each field and each material  
 180 property characterizing the considered medium are functions of both  $X$  and  
 181  $Y$ , with  $Y = \varepsilon_0^{-1} X$ . Roughly speaking, the dependence on  $X$  captures the  
 182 behavior of a given physical quantity over the largest length-scale, while the  
 183 dependence on  $Y$  captures the behavior over the smallest one. We express  
 184 this property by introducing the notation  $\Phi^\varepsilon(X) = \Phi(X, \varepsilon_0^{-1} X) = \Phi(X, Y)$   
 185 [66]. Moreover, for a fixed  $X$ , we assume that  $\Phi(X, Y)$  is periodic with  
 186 respect to  $Y$ .

187 In the classical theory of two-scale asymptotic homogenization [5, 8, 14],  
 188 the small scaling dimensionless parameter  $\varepsilon_0$  is constant. However, in the  
 189 case of a composite material subjected to deformation and change of internal  
 190 structure (as is the case, for instance, when plastic-like distortions occur),  
 191 the characteristic macroscopic and microscopic lengths, which refer to the  
 192 body and to its heterogeneities, respectively, depend on  $X$  and  $t$ , and should  
 193 thus be denoted by  $\ell(X, t)$  and  $L(X, t)$ . Therefore, the corresponding scaling  
 194 parameter, obtained as the ratio  $\varepsilon(X, t) = \ell(X, t)/L(X, t)$ , is also a func-  
 195 tion of  $X$  and  $t$ , which need not be equal to  $\varepsilon_0$  in general. This variability

196 notwithstanding, if  $\varepsilon(X, t)$  is bounded from above for all  $X$  and for all  $t$ , and  
 197 if the upper bound is much smaller than unity, we can indicate such upper  
 198 bound with  $\varepsilon$ , and use this constant scaling parameter for our asymptotic  
 199 analysis.

## 200 2.2. Kinematics

201 Let us denote by  $\mathcal{B}^\varepsilon$  a continuum body with periodic microstructure, and  
 202 by  $\mathcal{S}$  the three-dimensional Euclidean space. Furthermore, we denote by  
 203  $\mathcal{B}_0^\varepsilon$  the reference, unloaded configuration of  $\mathcal{B}^\varepsilon$ , in which the body's periodic  
 204 micro-structure is reproduced. Now, let us assume that  $\chi^\varepsilon : \mathcal{B}_0^\varepsilon \times \mathcal{T} \rightarrow \mathcal{S}$   
 205 describes the motion of the heterogeneous body, where  $\mathcal{T} = [t_0, t_f[$  is an  
 206 interval of time. Then, the region occupied by the body at time  $t \in \mathcal{T}$   
 207 is  $\mathcal{B}_t^\varepsilon := \chi^\varepsilon(\mathcal{B}_0^\varepsilon, t) \subset \mathcal{S}$  and is said to be its current configuration. Each  
 208 point  $x \in \mathcal{B}_t^\varepsilon$  is such that  $x = \chi^\varepsilon(X, t)$ , with  $X \in \mathcal{B}_0^\varepsilon$  being the point's  
 209 reference placement. The deformation from  $\mathcal{B}_0^\varepsilon$  to  $\mathcal{B}_t^\varepsilon$  is characterized by the  
 210 deformation gradient,  $\mathbf{F}^\varepsilon(X, t)$ , which is defined as  $\mathbf{F}^\varepsilon(X, t) = T\chi^\varepsilon(X, t)$   
 211 [53], with  $T\chi^\varepsilon$  being the map from the tangent space  $T_X\mathcal{B}_0^\varepsilon$  into  $T_x\mathcal{S}$ . In  
 212 the sequel, however, since our focus is on Homogenization Theory, we find it  
 213 convenient to use the less formal definition

$$\mathbf{F}^\varepsilon = \mathbf{I} + \text{Grad}\mathbf{u}^\varepsilon, \quad (4)$$

214 where  $\mathbf{I}$  is the second-order identity tensor and  $\text{Grad}\mathbf{u}^\varepsilon$  denotes the gradient  
 215 operator of the displacement  $\mathbf{u}^\varepsilon$ . The condition  $J^\varepsilon = \det\mathbf{F}^\varepsilon > 0$  must be  
 216 satisfied in order for  $\chi^\varepsilon$  to be admissible. The symmetric, positive definite,  
 217 second-order tensor  $\mathbf{C}^\varepsilon = (\mathbf{F}^\varepsilon)^T\mathbf{F}^\varepsilon$  is the right Cauchy-Green deformation  
 218 tensor induced by  $\mathbf{F}^\varepsilon$ . For our purposes, we partition  $\mathcal{B}_0^\varepsilon$  into two sub-  
 219 domains  $\mathcal{B}_0^1$  and  $\mathcal{B}_0^2$ , such that  $\bar{\mathcal{B}}_0^1 \cup \bar{\mathcal{B}}_0^2 = \bar{\mathcal{B}}_0^\varepsilon$  and  $\mathcal{B}_0^1 \cap \mathcal{B}_0^2 = \emptyset$ . We let  
 220  $\Gamma_0^\varepsilon$  stand for the interface between  $\mathcal{B}_0^1$  and  $\mathcal{B}_0^2$ . Particularly,  $\mathcal{B}_0^1$  denotes the  
 221 matrix of  $\mathcal{B}^\varepsilon$  (also referred to as *host phase*) and  $\mathcal{B}_0^2$  a collection of  $N$  disjoint  
 222 inclusions. The periodic cell in the reference configuration is denoted by  $\mathcal{Y}_0$ .  
 223 The portion of matrix contained in  $\mathcal{Y}_0$  is indicated by  $\mathcal{Y}_0^1$ , while  $\mathcal{Y}_0^2$  is the  
 224 inclusion in  $\mathcal{Y}_0$ . In each cell,  $\mathcal{Y}_0^1$  and  $\mathcal{Y}_0^2$  are such that  $\bar{\mathcal{Y}}_0^1 \cup \bar{\mathcal{Y}}_0^2 = \mathcal{Y}_0$  and  
 225  $\mathcal{Y}_0^1 \cap \mathcal{Y}_0^2 = \emptyset$ . The symbol  $\Gamma_0$  indicates the interface between  $\mathcal{Y}_0^1$  and  $\mathcal{Y}_0^2$ .  
 226 In the present work, we assume that the periodicity of the body's micro-  
 227 structure is preserved even though the body evolves by both changing its  
 228 shape and varying its internal structure. In general, however, this is not the  
 229 case. [Clearly, our hypothesis is unrealistic in several circumstances, but it](#)

230 might be helpful to describe those situations in which the breaking of the  
 231 material symmetries occurs at a scale different from those of interest, as is  
 232 the case, for instance, when the plastic distortions occur in a tissue with  
 233 evolving material properties [49], and are not directly related to the change  
 234 of the tissue’s micro-geometry. On the other hand, for nonperiodic media,  
 235 the macro model is still valid when one assumed local boundedness. In that  
 236 case, the coefficients are simply to be retrieved experimentally, as the “cell”  
 237 problem are no longer to be computed on the cell but, on the whole micro  
 238 domain, which would be more complex than the original problem.

239 Moreover, we define  $\chi_1^\varepsilon := \chi^\varepsilon|_{\mathcal{B}_0^1} : \mathcal{B}_0^1 \times \mathcal{T} \rightarrow \mathcal{S}$  such that  $\mathcal{B}_t^1 := \chi_1^\varepsilon(\mathcal{B}_0^1, t)$   
 240 denotes the host phase at the current configuration and  $\chi_2^\varepsilon := \chi^\varepsilon|_{\mathcal{B}_0^2} : \mathcal{B}_0^2 \times$   
 241  $\mathcal{T} \rightarrow \mathcal{S}$ , with  $\mathcal{B}_t^2 := \chi_2^\varepsilon(\mathcal{B}_0^2, t)$  denoting the inclusions. Specifically, we enforce  
 242 the condition  $\bar{\mathcal{B}}_t^1 \cup \bar{\mathcal{B}}_t^2 = \bar{\mathcal{B}}_t^\varepsilon$ , with  $\mathcal{B}_t^1 \cap \mathcal{B}_t^2 = \emptyset$ , and denote by  $\Gamma_t^\varepsilon$  the interface  
 243 between  $\mathcal{B}_t^1$  and  $\mathcal{B}_t^2$ . In addition, we let  $\mathcal{Y}_t$  indicate the periodic cell in the  
 244 current configuration, with  $\bar{\mathcal{Y}}_t^1 \cup \bar{\mathcal{Y}}_t^2 = \mathcal{Y}_t$ ,  $\mathcal{Y}_t^1 \cap \mathcal{Y}_t^2 = \emptyset$ , and with  $\Gamma_t$  being  
 245 the interface between  $\mathcal{Y}_t^1$  and  $\mathcal{Y}_t^2$  (see Fig. 1). We emphasize that  $\mathcal{Y}_t^1$  is the  
 246 portion of matrix and  $\mathcal{Y}_t^2$  is the inclusion in  $\mathcal{Y}_t$ . We note that inside a single  
 247 cell it can be present also a collection of inclusions and, in such a case, we  
 248 should consider multiple interface conditions [60].

### 249 2.3. Multiplicative decomposition

250 When the body  $\mathcal{B}^\varepsilon$  is subjected to a system of external loads, the change  
 251 of its shape could be accompanied by a rearrangement of its intrinsic struc-  
 252 ture. This process is generally inelastic and may not be associated to a de-  
 253 formation. Moreover, when mechanical agencies are removed, the body is  
 254 generally unable to recover the unloaded configuration  $\mathcal{B}_0^\varepsilon$ , and may occupy  
 255 a configuration characterized by the presence of residual stresses and strains.  
 256 To bring the body into a fully relaxed state, an ideal tearing process has to  
 257 be introduced [55]. More specifically, for each material point  $X \in \mathcal{B}^\varepsilon$ , we  
 258 individuate a small neighborhood of  $X$ , referred to as *body element*, we ide-  
 259 ally cut it out from the body, and we let it relax until it reaches a stress-free  
 260 state. Such state is the *ground state* of the relaxed body element and is called  
 261 *natural state*. This concept, originally used in the theory of elasto-plasticity  
 262 (see [50, 55]), has been used in the biomechanical context by various authors  
 263 like, for instance, [23, 76, 30, 26, 27, 42, 44, 18, 55, 34, 19]. Before going  
 264 further with the use of the BKL decomposition, we mention that, in the  
 265 literature, there exist other approaches to the issue of residual stresses in  
 266 biological tissues, which call neither for the multiplicative decomposition of

267 the deformation gradient tensor, nor for the introduction of an “intermediate,  
 268 relaxed configuration”. One recent publication adhering to this philosophy  
 269 is for example [13], in which the authors warn that the intermediate config-  
 270 uration may “*not exist in physical reality and must be postulated a priori*”.  
 271 Although we are aware of the fact that a framework based on the BKL-  
 272 decomposition may lead in some cases to assume unrealistic results —as any  
 273 other framework would do—, we prefer here to adhere to the BKL approach  
 274 for consistency of previous works of ours.

275 By performing the ideal process described above for all the body points, a  
 276 collection of relaxed body pieces is obtained, in which each piece finds itself  
 277 in its natural state. We denote such collection by  $\mathcal{B}_\nu^\varepsilon$ . In the language of  
 278 continuum mechanics, these physical considerations lead to the BKL decom-  
 279 position [55, 34]. Although summarizing these theoretical results is useful for  
 280 sake of completeness, the BKL decomposition is one the pillars of Elastoplas-  
 281 ticity, and so, its consequences are well-known. For this reason, we do not  
 282 fuss over its theoretical justification, and we highlight, rather, the fact that  
 283 one of the purposes of this work is to investigate the use of a scale-dependent  
 284 BKL decomposition. In detail, by referring to Figure 1, we invoke a multi-  
 285 plicative decomposition of the deformation gradient  $\mathbf{F}^\varepsilon$  that is parameterized  
 286 by the scaling ratio  $\varepsilon$ , i.e.,

$$\mathbf{F}^\varepsilon = \mathbf{F}_e^\varepsilon \mathbf{F}_p^\varepsilon, \quad (5)$$

287 where the tensor  $\mathbf{F}_e^\varepsilon$  and  $\mathbf{F}_p^\varepsilon$  describe, respectively, the elastic and the in-  
 288 elastic distortions contributing to  $\mathbf{F}^\varepsilon$ . Consistently with the notation intro-  
 289 duced above, it holds true that  $\mathbf{F}_e^\varepsilon(X) = \mathbf{F}_e(X, Y)$ ,  $\mathbf{F}_p^\varepsilon(X) = \mathbf{F}_p(X, Y)$ , and  
 290  $\mathbf{F}^\varepsilon(X) = \mathbf{F}(X, Y)$ .

291 In this work, we focus on remodeling, i.e., plastic-like distortions that  
 292 occur to modify the internal structure of  $\mathcal{B}^\varepsilon$ . Although this phenomenon is  
 293 not visible, it could lead to the alteration of the mechanical properties of  $\mathcal{B}^\varepsilon$ .

### 294 3. Formulation of the problem

295 We consider a composite material comprising two solid constituents, whose  
 296 point-wise constitutive response is hyperelastic. Therefore, to model its me-  
 297 chanical behavior, we introduce the scale-dependent strain energy function,  
 298 defined per unit volume of the natural state,

$$\check{\psi}_\nu(X, t) = \psi_\nu^\varepsilon(\mathbf{F}_e^\varepsilon(X, t), i^\varepsilon(X, t)) = \psi_\nu(\mathbf{F}_e(X, Y, t), i(X, Y, t)), \quad (6)$$

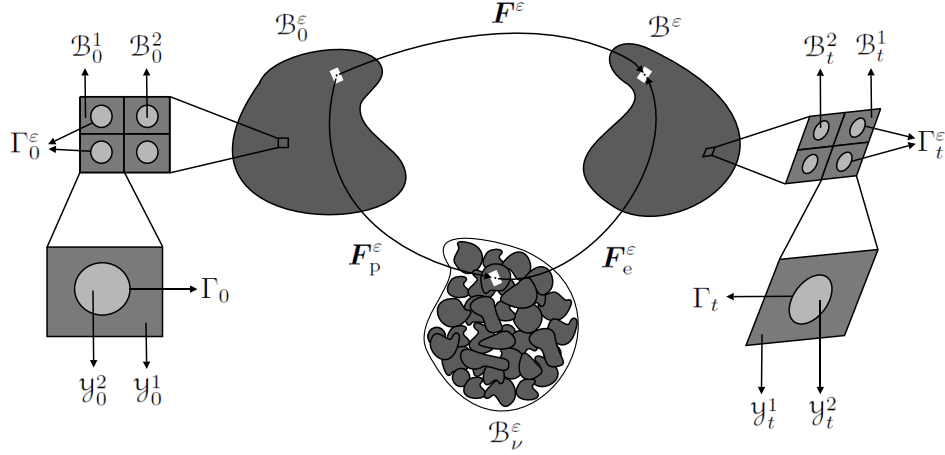


Figure 1: [Schematic](#) of a composite material with periodic internal micro-structure and subjected to inelastic remodeling distortions. From left to right: Magnification of an excerpt of material and description of its nested, periodic micro-structure. Change of shape of the body from the reference to the current configuration, and definition of the conglomerate of relaxed body pieces, each in its natural state. Magnification of an excerpt of material, taken from the body's current configuration, and description of its deformed, and remodeled, micro-structure.

299 where  $i$  is defined by the expression  $i(X, Y, t) = (X, Y)$ , i.e.,  $i$  extracts the  
 300 spatial pair  $(X, Y)$  from the triplet  $(X, Y, t)$ . From (6) we can derive the first  
 301 Piola-Kirchhoff stress tensor,

$$\mathbf{T}^\epsilon = J_p^\epsilon \frac{\partial \psi_\nu^\epsilon}{\partial \mathbf{F}_p^\epsilon} (\mathbf{F}_p^\epsilon)^{-T}, \quad (7)$$

302 where  $J_p^\epsilon = \det \mathbf{F}_p^\epsilon$ . In particular, if we neglect body forces and inertial terms,  
 303 the balance of linear momentum reads,

$$\begin{cases} \text{Div } \mathbf{T}^\epsilon = \mathbf{0}, & \text{in } \mathcal{B}_0^\epsilon \setminus \Gamma_0^\epsilon \times \mathcal{T}, \\ \mathbf{T}^\epsilon \cdot \mathbf{N} = \bar{\mathbf{T}}, & \text{on } \partial_T \mathcal{B}_0^\epsilon \times \mathcal{T}, \\ \mathbf{u}^\epsilon = \bar{\mathbf{u}}, & \text{on } \partial_u \mathcal{B}_0^\epsilon \times \mathcal{T}, \end{cases} \quad (8)$$

304 where  $\bar{\mathbf{T}}$  and  $\bar{\mathbf{u}}$  are, respectively, the prescribed traction and displacement  
 305 on the boundary  $\partial \mathcal{B}_0^\epsilon = \partial_T \mathcal{B}_0^\epsilon \cup \partial_u \mathcal{B}_0^\epsilon$  with  $\partial_T \mathcal{B}_0^\epsilon \cap \partial_u \mathcal{B}_0^\epsilon = \emptyset$  and  $\mathbf{N}$  is the  
 306 outward unit vector normal to the surface  $\partial \mathcal{B}_0^\epsilon$ . Continuity conditions for  
 307 displacement and traction are imposed,

$$[[\mathbf{u}^\epsilon]] = \mathbf{0} \quad \text{and} \quad [[\mathbf{T}^\epsilon \cdot \mathbf{N}_y]] = \mathbf{0} \quad \text{on } \Gamma_0 \times \mathcal{T}, \quad (9)$$

308 where  $\llbracket \bullet \rrbracket$  denotes the jump across the interface between the two constituents  
 309 and  $\mathbf{N}_y$  defines the unit outward normal to  $\Gamma_0$ . Moreover, problem (8) must  
 310 be supplemented with an appropriate evolution law for  $\mathbf{F}_p^\varepsilon$ . It is worth men-  
 311 tioning that the homogenization process can be performed regardless on the  
 312 particular choice of *external* (Dirichlet-Neumann in this case) boundary con-  
 313 ditions. This means that the formulation presented in this work is potentially  
 314 applicable also to other external boundary conditions, such as e.g. those of  
 315 Robin-type. This is due to the fact that, as pointed out in [69], also in the  
 316 present study the homogenization is applied in regions sufficiently far away  
 317 from the outer boundary of the considered medium. For problems in which it  
 318 is necessary to homogenize also close to the outer heterogeneous boundaries,  
 319 we refer to [8, 57, 46].

320 **Remark 1.** *In the present work, we impose conditions (9) for displacements*  
 321 *and tractions just to exemplify the homogenization technique applied to het-*  
 322 *erogeneous media with evolving microstructure. In other words, we assume*  
 323 *that the contact interface between the constituents is ideal. This means that*  
 324 *the displacements are congruent, and thus continuous, and that linear mo-*  
 325 *mentum is conserved across the interface, which in our context, implies the*  
 326 *continuity of the tractions. However, the hypothesis of the ideal interface can*  
 327 *be relaxed in some biological situations. For instance, in cancerous tissues,*  
 328 *there exist cross-links between normal and malignant cells, whose density and*  
 329 *strength determine a spring constant that relates the normal stresses on each*  
 330 *cell surface, thereby making it non-ideal [47, 37]. Another example of non-*  
 331 *ideal interface is the periodontal ligament, which represents the thin layer*  
 332 *between the cementum of the tooth to the adjacent alveolar bone [28]. In the*  
 333 *context of composite materials, when non-ideal interfaces are accounted for,*  
 334 *the interface conditions are suitably reformulated [38, 39, 7, 6]. In particular,*  
 335 *the asymptotic homogenization technique has been applied for linear elastic*  
 336 *periodic fiber reinforced composites with imperfect contact between matrix and*  
 337 *fibers (see e.g. [36]).*

#### 338 4. Asymptotic homogenization of the balance of linear momentum

339 A formal two-scale asymptotic expansion is performed for the displace-  
 340 ment  $\mathbf{u}^\varepsilon$ , which thus reads

$$\mathbf{u}^\varepsilon(X, t) = \mathbf{u}^{(0)}(X, t) + \sum_{k=1}^{+\infty} \mathbf{u}^{(k)}(X, Y, t) \varepsilon^k, \quad (10)$$

341 where, for all  $k \geq 1$ ,  $\mathbf{u}^{(k)}$  is periodic with respect to  $Y$ . Following [68] we  
 342 consider the leading order term of the expansion (10) to be independent of  
 343 the fast variable  $Y$ . From formula (4), the expansion (10), and taking into  
 344 account the property of scales separation, it follows that the deformation  
 345 gradient tensor can be written as

$$\mathbf{F}^\varepsilon(X, t) = \sum_{k=0}^{+\infty} \mathbf{F}^{(k)}(X, Y, t) \varepsilon^k, \quad (11)$$

346 with the notation

$$\mathbf{F}^{(0)} := \mathbf{I} + \text{Grad}_X \mathbf{u}^{(0)} + \text{Grad}_Y \mathbf{u}^{(1)}, \quad (12a)$$

$$\mathbf{F}^{(k)} := \text{Grad}_X \mathbf{u}^{(k)} + \text{Grad}_Y \mathbf{u}^{(k+1)}, \quad \forall k \geq 1. \quad (12b)$$

347 where  $\text{Grad}_X$  and  $\text{Grad}_Y$  are the gradient operators with respect to  $X$  and  $Y$ ,  
 348 respectively. Now, the following two-scale asymptotic expansion is proposed  
 349 for the first Piola-Kirchhoff stress tensor  $\mathbf{T}^\varepsilon$ ,

$$\mathbf{T}^\varepsilon(X, t) = \sum_{k=0}^{+\infty} \mathbf{T}^{(k)}(X, Y, t) \varepsilon^k, \quad (13)$$

350 where the fields  $\mathbf{T}^{(k)}$  are periodic with respect to  $Y$ . By substituting the  
 351 power series representation (13) into (8), using the scales separation con-  
 352 dition, and multiplying the result by  $\varepsilon$ , the following multi-scale system is  
 353 obtained

$$\text{Div} \mathbf{T}^\varepsilon = \sum_{k=0}^{+\infty} \mathfrak{D}^{(k)} \varepsilon^k = \mathbf{0}, \quad (14)$$

354 with

$$\mathfrak{D}^{(0)} := \text{Div}_Y \mathbf{T}^{(0)}, \quad (15a)$$

$$\mathfrak{D}^{(k)} := \text{Div}_X \mathbf{T}^{(k-1)} + \text{Div}_Y \mathbf{T}^{(k)}, \quad \forall k \geq 1. \quad (15b)$$

355 We require that the equilibrium equation (14) is satisfied at every  $\varepsilon$ , which  
 356 amounts to impose the conditions

$$\text{Div}_Y \mathbf{T}^{(0)} = \mathbf{0} \quad (16a)$$

$$\text{Div}_X \mathbf{T}^{(k-1)} + \text{Div}_Y \mathbf{T}^{(k)} = \mathbf{0}, \quad \forall k \geq 1. \quad (16b)$$

357 At this point we introduce the average operator over the microscopic cell, i.e.

$$\langle \bullet \rangle = \frac{1}{|\mathcal{Y}_t|} \int_{\mathcal{Y}_t} \bullet \, dY, \quad (17)$$

358 where  $|\mathcal{Y}_t|$  represents the volume of the periodic cell  $\mathcal{Y}_t$  at time  $t$ . Indeed,  
 359 because of the deformations and distortions to which the microscopic, refer-  
 360 ence periodic cell is subjected,  $\mathcal{Y}_t$  is different at every time instant. Averaging  
 361 (16b) over the microscopic cell yields, for  $k = 1$ ,

$$\langle \text{Div}_X \mathbf{T}^{(0)} \rangle + \frac{1}{|\mathcal{Y}_t|} \int_{\partial \mathcal{Y}_t} \mathbf{T}^{(1)} \cdot \mathbf{N} \, dY = \mathbf{0}, \quad (18)$$

362 where, on the left-hand side, we have applied the divergence theorem. Since  
 363 the contributions on the periodic cell boundary  $\partial \mathcal{Y}$  cancel due to the  $Y$ -  
 364 periodicity, the integral over  $\mathcal{Y}_t$  is equal to zero, and (18) becomes

$$\langle \text{Div}_X \mathbf{T}^{(0)} \rangle = \mathbf{0}. \quad (19)$$

365 Here, we restrict our analysis to the particular case in which the periodic  
 366 cell can be uniquely chosen independently of  $X$ , which implies that the in-  
 367 tegration over  $\mathcal{Y}_t$  and the computation of the divergence commute. This  
 368 assumption is also referred to as *macroscopic uniformity*, see also [9, 40, 59]  
 369 for example dealing with non-macroscopically uniform media in the context  
 370 of poroelasticity and diffusion. Therefore, Equation (19) can be recast as

$$\text{Div}_X \langle \mathbf{T}^{(0)} \rangle = \mathbf{0}. \quad (20)$$

371 Equations (16a) and (20) represent, respectively, the local and the homoge-  
 372 nized equation associated with the original one, stated in (8). Both equations  
 373 still need to be supplemented with the corresponding interface, boundary, and  
 374 initial conditions. Note that, although both problems feature no time deriva-  
 375 tive, initial conditions are required because  $\mathbf{T}^{(0)}$  depends on the variable  $\mathbf{F}_p^{(0)}$ ,  
 376 which satisfies an evolution equation in time.

377 We remark that the leading term  $\mathbf{T}^{(0)} = \mathbf{T}^{(0)}(X, Y, t)$  of the multi-scale  
 378 expansion (13) is the unknown, both in (16a) and in (20). To identify  $\mathbf{T}^{(0)}$ ,  
 379 we propose here to expand  $\mathbf{F}_p^\varepsilon$  and  $\psi_\nu^\varepsilon$  as

$$\mathbf{F}_p^\varepsilon(X, t) = \sum_{k=0}^{+\infty} \mathbf{F}_p^{(k)}(X, Y, t) \varepsilon^k, \quad (21a)$$

$$\psi_\nu^\varepsilon(X, t) = \sum_{k=0}^{+\infty} \psi_\nu^{(k)}(\mathbf{F}_e(X, Y, t), X, Y) \varepsilon^k, \quad (21b)$$

380 where  $\mathbf{F}_p^{(k)}$  and  $\psi_\nu^{(k)}$  are periodic in  $Y$  for all  $k \geq 1$ . By using (5), (11) and  
 381 (21a), we can deduce a series expansion for  $\mathbf{F}_e^\varepsilon$  in powers of  $\varepsilon$ , where the  
 382 leading order term  $\mathbf{F}_e^{(0)}$  is given by

$$\mathbf{F}_e^{(0)} = \mathbf{F}^{(0)}(\mathbf{F}_p^{(0)})^{-1}. \quad (22)$$

383 Following [15] and [68],  $\mathbf{T}^{(0)}$  is therefore supplied constitutively as

$$\mathbf{T}^{(0)} = J_p^{(0)} \frac{\partial \psi_\nu^{(0)}}{\partial \mathbf{F}_e^{(0)}} (\mathbf{F}_p^{(0)})^{-T}, \quad (23)$$

384 with  $\psi_\nu^{(0)} = \psi_\nu^{(0)}(\mathbf{F}_e^{(0)}(X, Y, t), X, Y)$  and  $J_p^{(0)} = \det \mathbf{F}_p^{(0)}$ . To obtain the  
 385 *cell problem*, equation (14) must be supplemented with the corresponding  
 386 interface conditions. This is done by substituting the asymptotic expansions  
 387 of  $\mathbf{u}^\varepsilon$  and of  $\mathbf{T}^\varepsilon$  into the interface conditions  $[[\mathbf{u}^\varepsilon]] = \mathbf{0}$  and  $[[\mathbf{T}^\varepsilon \cdot \mathbf{N}_y]] = \mathbf{0}$ .  
 388 Both conditions are satisfied at any order of  $\varepsilon$ . At the order  $\varepsilon^0$ , we simply  
 389 obtain  $[[\mathbf{T}^{(0)} \cdot \mathbf{N}_y]] = \mathbf{0}$  for the stresses, and that the condition  $[[\mathbf{u}^{(0)}]] = \mathbf{0}$   
 390 is trivially satisfied, because  $\mathbf{u}^{(0)}$  depends solely on  $X$  and  $t$ . Thus, the interface  
 391 condition on the displacements is written only for  $\mathbf{u}^{(1)}$  and reads,  $[[\mathbf{u}^{(1)}]] = \mathbf{0}$ .  
 392 By summarizing these results, the cell problem at zero order of the epsilon  
 393 parameter can be stated as

$$\begin{cases} \text{Div}_Y \mathbf{T}^{(0)} = \mathbf{0}, & \text{in } \mathcal{Y}_0 \setminus \Gamma_0 \times \mathcal{T}, \\ [[\mathbf{u}^{(1)}]] = \mathbf{0}, & \text{on } \Gamma_0 \times \mathcal{T}, \\ [[\mathbf{T}^{(0)} \cdot \mathbf{N}_y]] = \mathbf{0}, & \text{on } \Gamma_0 \times \mathcal{T}. \end{cases} \quad (24)$$

394 Together with the cell problem, we also need to formulate the macro-scopic  
 395 homogenized problem. To this end, we take equation (20) and complete it  
 396 with a set of boundary conditions. This is done by substituting the asymp-  
 397 totic expansions of  $\mathbf{T}^\varepsilon$  and  $\mathbf{u}^\varepsilon$  into the boundary conditions  $\mathbf{T}^\varepsilon \cdot \mathbf{N} = \bar{\mathbf{T}}$   
 398 and  $\mathbf{u}^\varepsilon = \bar{\mathbf{u}}$ , respectively. Thus, equating the coefficients at order  $\varepsilon^0$ , and  
 399 averaging the results over the unit cell, we find the *homogenized problem*,

$$\begin{cases} \text{Div}_X \langle \mathbf{T}^{(0)} \rangle = \mathbf{0}, & \text{in } \mathcal{B}_h \times \mathcal{T}, \\ \langle \mathbf{T}^{(0)} \rangle \cdot \mathbf{N} = \bar{\mathbf{T}}, & \text{on } \partial_T \mathcal{B}_h \times \mathcal{T}, \\ \mathbf{u}^{(0)} = \bar{\mathbf{u}}, & \text{on } \partial_u \mathcal{B}_h \times \mathcal{T}, \end{cases} \quad (25)$$

400 where  $\mathcal{B}_h$  denotes the homogeneous macro-scale domain in which the homog-  
 401 enized equations are defined.

402 The problem (25) has to be solved along with a homogenized evolution  
 403 equation for  $\mathbf{F}_p^{(0)}$  and the initial condition associated with it. In addition, we  
 404 remark that, according to (25), the boundary tractions acting on  $\partial_T \mathcal{B}_h$  are  
 405 balanced *only* by the normal component of the average of the leading order  
 406 stress,  $\mathbf{T}^{(0)}$ , and *only* the leading order displacement,  $\mathbf{u}^{(0)}$ , has to be equal  
 407 to the displacement  $\bar{\mathbf{u}}$ , imposed on  $\partial_u \mathcal{B}_h$ .

408 **Remark 2.** *In the medical scientific literature, there exist studies that iden-*  
 409 *tify the existence of anatomical boundary layers interposed between the brain*  
 410 *surface and tumors (see e.g. [72]). Here we do not address boundary layer*  
 411 *phenomena, which is usually neglected in the asymptotic homogenization lit-*  
 412 *erature. The homogenization process described in this work is fine for regions*  
 413 *far enough away from the boundary so that its effect is not felt because near*  
 414 *boundaries the material will not behave as an effective material with homog-*  
 415 *enized coefficients. To properly account for boundary effects, the so-called*  
 416 *boundary-layer technique could be used [8, 57].*

## 417 5. Constitutive framework and evolution law

418 In this section, we prescribe a constitutive equation for the response of the  
 419 material and, independently, an evolution equation for the tensor of plastic-  
 420 like distortions.

### 421 5.1. Constitutive law

422 In the following, we formulate the local and homogenized problems for a  
 423 specific constitutive law. In general, this process can be rather cumbersome  
 424 for complicated strain energy densities, and it becomes even more involved  
 425 when plastic-like distortions are accounted for. To reduce complexity, we  
 426 choose a very simple constitutive law for  $\psi_\nu^\varepsilon$ , such as the De Saint-Venant  
 427 strain energy density,

$$\psi_\nu^\varepsilon = \frac{1}{2} \mathbf{E}_e^\varepsilon : \mathcal{C}^\varepsilon : \mathbf{E}_e^\varepsilon, \quad (26)$$

428 where  $\mathbf{E}_e^\varepsilon = \frac{1}{2}(\mathbf{C}_e^\varepsilon - \mathbf{I})$  is the elastic Green-Lagrange strain tensor and  
 429  $\mathcal{C}^\varepsilon(X) = \mathcal{C}(X, Y)$  is the positive definite fourth-order elasticity tensor, which

430 satisfies both major and minor symmetries, i.e.  $\mathcal{C}_{ijkl} = \mathcal{C}_{jikl} = \mathcal{C}_{ijlk} = \mathcal{C}_{klij}$ .  
 431 Particularly, we consider that the constituents of the heterogeneous material  
 432 are isotropic, and thus

$$\mathcal{C}^\varepsilon = 3\kappa^\varepsilon \mathcal{K} + 2\mu^\varepsilon \mathcal{M}, \quad (27)$$

433 where  $\kappa^\varepsilon(X) = \kappa(X, Y)$  is the bulk modulus,  $\mu^\varepsilon(X) = \mu(X, Y)$  is the shear  
 434 modulus, and the fourth-order tensors  $\mathcal{K} = \frac{1}{3}(\mathbf{I} \otimes \mathbf{I})$  and  $\mathcal{M} = \mathcal{I} - \mathcal{K}$   
 435 extract the spherical and the deviatoric part, respectively, of a symmetric  
 436 second-order tensor  $\mathbf{A}$ , i.e.,  $\mathcal{K} : \mathbf{A} = \frac{1}{3}\text{tr}(\mathbf{A})\mathbf{I}$  and  $\mathcal{M} : \mathbf{A} = \mathbf{A} - \frac{1}{3}\text{tr}(\mathbf{A})\mathbf{I} :=$   
 437  $\text{dev}(\mathbf{A})$  [84, 85]. We remark that the fourth-order identity tensor  $\mathcal{I}$  is the  
 438 identity operator over the linear subspace of symmetric second-order tensors.  
 439 Indeed, for every  $\mathbf{A}$  such that  $\mathbf{A} = \mathbf{A}^T$ , it holds that  $\mathcal{I} : \mathbf{A} = \mathbf{A}$ . In  
 440 terms of  $\mathbf{I}$ , an explicit expression of  $\mathcal{I}$  is given by  $\mathcal{I} = \frac{1}{2}[\mathbf{I} \otimes \mathbf{I} + \mathbf{I} \overline{\otimes} \mathbf{I}]$  (in  
 441 components:  $\mathcal{I}_{ijkl} = \frac{1}{2}[I_{ik}I_{jl} + I_{il}I_{jk}]$  [17]).

442 We can identify the leading order term in the expansion of the constitutive  
 443 law (26), which reads

$$\psi_\nu^{(0)} = \frac{1}{2} \mathbf{E}_e^{(0)} : \mathcal{C} : \mathbf{E}_e^{(0)}, \quad (28)$$

444 with  $\mathbf{E}_e^{(0)} = \frac{1}{2}(\mathbf{C}_e^{(0)} - \mathbf{I})$ . We recall that, although the expression of  $\psi_\nu^{(0)}$   
 445 in (28) depends only on  $\mathbf{E}_e^{(0)}$ , the material coefficient  $\mathcal{C}$  is still a two-scale  
 446 function and should be thus interpreted as  $\mathcal{C}(X, Y)$ . As a consequence,  $\psi_\nu^{(0)}$   
 447 is not homogenized yet.

448 By taking into account the major and minor symmetries of  $\mathcal{C}$ , we obtain

$$\mathbf{S}_\nu^{(0)} = \frac{\partial \psi_\nu^{(0)}}{\partial \mathbf{E}_e^{(0)}} = \mathcal{C} : \mathbf{E}_e^{(0)} = \lambda \text{tr}(\mathbf{E}_e^{(0)})\mathbf{I} + 2\mu \mathbf{E}_e^{(0)}, \quad (29)$$

449 where  $\mathbf{S}_\nu^{(0)}$  is the leading order term of the second Piola-Kirchhoff stress  
 450 tensor written with respect to the natural state,  $\lambda = \kappa - \frac{2}{3}\mu$  is Lamé's  
 451 constant, and  $\mathbf{E}_e^{(0)}$  is given by

$$\mathbf{E}_e^{(0)} = (\mathbf{F}_p^{(0)})^{-T} \left( \mathbf{E}^{(0)} - \mathbf{E}_p^{(0)} \right) (\mathbf{F}_p^{(0)})^{-1}, \quad (30)$$

452 with  $\mathbf{E}^{(0)} = \frac{1}{2} \left( (\mathbf{F}^{(0)})^T \mathbf{F}^{(0)} - \mathbf{I} \right)$  and  $\mathbf{E}_p^{(0)} = \frac{1}{2} \left( (\mathbf{F}_p^{(0)})^T \mathbf{F}_p^{(0)} - \mathbf{I} \right)$ .

453 By pulling  $\mathbf{S}_\nu^{(0)}$  back to the reference configuration, and recalling that the  
 454 plastic-like distortions are assumed to be isochoric in our framework, (i.e.  
 455  $J_p^\varepsilon = 1$ ), we obtain the second Piola-Kirchhoff stress tensor

$$\mathbf{S}^{(0)} = \mathcal{C}_R : (\mathbf{E}^{(0)} - \mathbf{E}_p^{(0)}), \quad (31)$$

456 where

$$\begin{aligned} \mathcal{C}_R &= (\mathbf{F}_p^{(0)})^{-1} \otimes (\mathbf{F}_p^{(0)})^{-1} : \mathcal{C} : (\mathbf{F}_p^{(0)})^{-T} \otimes (\mathbf{F}_p^{(0)})^{-T} \\ &= 3\lambda \mathcal{K}_p^{(0)} + 2\mu \mathcal{I}_p^{(0)}, \end{aligned} \quad (32)$$

457 is the elasticity tensor pulled-back to the reference configuration through  
 458  $\mathbf{F}_p^{(0)}$ , and, upon setting  $\mathbf{B}_p^{(0)} = (\mathbf{F}_p^{(0)})^{-1}(\mathbf{F}_p^{(0)})^{-T}$ , we employed the notation

$$\mathcal{K}_p^{(0)} = \frac{1}{3} \mathbf{B}_p^{(0)} \otimes \mathbf{B}_p^{(0)}, \quad (33a)$$

$$\mathcal{I}_p^{(0)} = \frac{1}{2} \left[ \mathbf{B}_p^{(0)} \underline{\otimes} \mathbf{B}_p^{(0)} + \mathbf{B}_p^{(0)} \overline{\otimes} \mathbf{B}_p^{(0)} \right]. \quad (33b)$$

459 We remark that  $\mathcal{K}_p^{(0)}$  extracts the ‘‘volumetric part’’ of a generic second-order  
 460 tensor, taken with respect to the inverse plastic metric tensor  $\mathbf{B}_p^{(0)} = (\mathbf{C}_p^{(0)})^{-1}$   
 461 i.e. for all  $\mathbf{A} = \mathbf{A}^T$ , it holds that  $\mathcal{K}_p^{(0)} : \mathbf{A} = \frac{1}{3} \text{tr}(\mathbf{B}_p^{(0)} \mathbf{A}) \mathbf{B}_p^{(0)}$ . Furthermore,  
 462  $\mathcal{I}_p^{(0)}$  transforms  $\mathbf{A}$  into  $\mathcal{I}_p^{(0)} : \mathbf{A} = \mathbf{B}_p^{(0)} \mathbf{A} \mathbf{B}_p^{(0)}$  and  $\mathcal{M}_p^{(0)} = \mathcal{I}_p^{(0)} - \mathcal{K}_p^{(0)}$   
 463 extracts the ‘‘deviatoric part’’ of  $\mathbf{A}$  with respect to the metric tensor  $\mathbf{B}_p^{(0)}$ ,  
 464 i.e.  $\mathcal{M}_p^{(0)} : \mathbf{A} = \mathbf{B}_p^{(0)} \mathbf{A} \mathbf{B}_p^{(0)} - \frac{1}{3} \text{tr}(\mathbf{B}_p^{(0)} \mathbf{A}) \mathbf{B}_p^{(0)}$ . We note that similar results  
 465 have been obtained in the case of non-linear elasticity in [25].

466 Next, we notice that  $\mathbf{F}^{(0)}$  can be written as

$$\mathbf{F}^{(0)} = \mathbf{I} + \mathbf{H}, \quad (34)$$

467 with  $\mathbf{H} = \text{Grad}_X \mathbf{u}^{(0)} + \text{Grad}_Y \mathbf{u}^{(1)}$ . Thus, by substituting (34) in  $\mathbf{E}_e^{(0)}$ ,  
 468 the result into (31), and retaining only the terms linear in  $\mathbf{H}$ ,  $\mathbf{S}^{(0)}$  can be  
 469 linearized as

$$\mathbf{S}_{\text{lin}}^{(0)} = \mathcal{C}_R : (\text{sym} \mathbf{H} - \mathbf{E}_p^{(0)}). \quad (35)$$

470 We recall now that, at the leading order, the first Piola-Kirchhoff stress tensor  
 471 reads  $\mathbf{T}^{(0)} = \mathbf{F}^{(0)} \mathbf{S}^{(0)}$ . Hence, its linearized form is given by

$$\mathbf{T}_{\text{lin}}^{(0)} = \mathcal{C}_R : \text{sym} \mathbf{H} - (\mathbf{I} + \mathbf{H})(\mathcal{C}_R : \mathbf{E}_p^{(0)}). \quad (36)$$

472 Looking at the definition of  $\mathcal{C}_R$  in (31), it can be noticed that our model re-  
 473 solves at the macro-scale the structural evolution of the considered medium  
 474 through the dependence of  $\mathcal{C}_R$  on  $\mathbf{F}_p^{(0)}$ , which indeed describes the produc-  
 475 tion of material inhomogeneities [21, 22, 23]. Additionally, our model is also  
 476 capable of simultaneously resolving the material heterogeneities at both the  
 477 micro- and macro-scale through the dependence of  $\mathcal{C}_R$  on  $X$  and  $Y$ . The lat-  
 478 ter dependence in fact, keeps track of the variability of the elastic coefficient  
 479 at both scales.

480 Because of Equations (33a) and (33b),  $\mathcal{C}_R$  possesses the same symmetry  
 481 properties of  $\mathcal{C}$ , i.e.

$$(\mathcal{C}_R)_{ijkl} = (\mathcal{C}_R)_{jikl} = (\mathcal{C}_R)_{ijlk} = (\mathcal{C}_R)_{klij}, \quad (37)$$

482 and therefore,  $\mathbf{T}_{\text{lin}}^{(0)}$  rewrites as

$$\mathbf{T}_{\text{lin}}^{(0)} = \mathcal{C}_R : \mathbf{H} - (\mathbf{I} + \mathbf{H})(\mathcal{C}_R : \mathbf{E}_p^{(0)}). \quad (38)$$

483 *Local problem.* Substituting (38) in the equation of the local problem (24),  
 484 the linear momentum balance law is rephrased as

$$\text{Div}_Y [\mathcal{C}_R : \mathbf{H} - (\mathbf{I} + \mathbf{H})(\mathcal{C}_R : \mathbf{E}_p^{(0)})] = \mathbf{0}, \quad (39)$$

485 or, equivalently,

$$\begin{aligned} & \text{Div}_Y [\mathcal{C}_R : \text{Grad}_Y \mathbf{u}^{(1)} - \text{Grad}_Y \mathbf{u}^{(1)} (\mathcal{C}_R : \mathbf{E}_p^{(0)})] = \\ & - \text{Div}_Y [\mathcal{C}_R : \text{Grad}_X \mathbf{u}^{(0)} - (\mathbf{I} + \text{Grad}_X \mathbf{u}^{(0)}) (\mathcal{C}_R : \mathbf{E}_p^{(0)})] \end{aligned} \quad (40)$$

486 In the absence of plastic distortions, i.e., when  $\mathbf{F}_p^\varepsilon = \mathbf{I}$ , Equation (40) coin-  
 487 cides with the equation of the classical cell problem encountered in the ho-  
 488 mogeneization of linear elasticity, which is known to admit a unique solution,  
 489 up to a  $Y$ -constant function, if the average over the cell of the right-hand-side  
 490 vanishes identically (in the jargon of Homogenization Theory, this condition  
 491 is referred to as *solvability condition* or *compatibility condition*) [5]. In our  
 492 case, since the pulled-back elasticity tensor  $\mathcal{C}_R$  is periodic in  $Y$ , while  $\mathbf{u}^{(0)}$  is  
 493 independent of  $Y$ , the solvability condition is satisfied, i.e.,

$$\langle \text{Div}_Y [\mathcal{C}_R : \text{Grad}_X \mathbf{u}^{(0)} - (\mathbf{I} + \text{Grad}_X \mathbf{u}^{(0)}) (\mathcal{C}_R : \mathbf{E}_p^{(0)})] \rangle = \mathbf{0}. \quad (41)$$

494 Exploiting the linearity of equation (40) in  $\mathbf{u}^{(1)}$ , we make the *ansatz*

$$\mathbf{u}^{(1)}(X, Y, t) = \boldsymbol{\xi}(X, Y, t) : \text{Grad}_X \mathbf{u}^{(0)}(X, t) + \boldsymbol{\omega}(X, Y, t), \quad (42)$$

495 where  $\boldsymbol{\xi}$  and  $\boldsymbol{\omega}$  are a third-order tensor function and a vector field, both  
 496 periodic in  $Y$ .

497 We now require that  $\boldsymbol{\xi}$  and  $\boldsymbol{\omega}$  satisfy two independent cell problems. The  
 498 cell problem for  $\boldsymbol{\xi}$  reads

$$\left\{ \begin{array}{ll} \text{Div}_Y [\mathcal{C}_R : T\text{Grad}_Y \boldsymbol{\xi} - T\text{Grad}_Y \boldsymbol{\xi}(\mathcal{C}_R : \mathbf{E}_p^{(0)})] \\ \quad = \text{Div}_Y [-\mathcal{C}_R + \mathbf{I} \otimes (\mathcal{C}_R : \mathbf{E}_p^{(0)})], & \text{in } \mathcal{Y}_0 \setminus \Gamma_0 \times \mathcal{T}, \\ \llbracket \boldsymbol{\xi} \rrbracket = \mathbf{0}, & \text{on } \Gamma_0 \times \mathcal{T}, \\ \llbracket [\mathcal{C}_R : T\text{Grad}_Y \boldsymbol{\xi} - T\text{Grad}_Y \boldsymbol{\xi}(\mathcal{C}_R : \mathbf{E}_p^{(0)}) \\ \quad + \mathcal{C}_R - \mathbf{I} \otimes (\mathcal{C}_R : \mathbf{E}_p^{(0)})] \cdot \mathbf{N}_Y \rrbracket = \mathbf{0}, & \text{on } \Gamma_0 \times \mathcal{T}. \end{array} \right. \quad (43)$$

499 Before going further, some words of explanation on the notation are nec-  
 500 essary. First, we notice that  $\text{Grad}_Y \boldsymbol{\xi}$  is a fourth-order tensor function, which  
 501 admits the representation  $\text{Grad}_Y \boldsymbol{\xi} = (\partial \xi_{ABC}) / (\partial Y_D) \mathbf{e}_A \otimes \mathbf{e}_B \otimes \mathbf{e}_C \otimes \mathbf{e}_D$ . Then,  
 502  $T\text{Grad}_Y \boldsymbol{\xi}$  is a fourth-order tensor function obtained by ordering the indices  
 503 of  $\text{Grad}_Y \boldsymbol{\xi}$  in the following fashion

$$\begin{aligned} T\text{Grad}_Y \boldsymbol{\xi} &= (T\text{Grad}_Y \boldsymbol{\xi})_{ABCD} \mathbf{e}_A \otimes \mathbf{e}_B \otimes \mathbf{e}_C \otimes \mathbf{e}_D \\ &= (\text{Grad}_Y \boldsymbol{\xi})_{ACDB} \mathbf{e}_A \otimes \mathbf{e}_B \otimes \mathbf{e}_C \otimes \mathbf{e}_D \\ &= \frac{\partial \xi_{ACD}}{\partial Y_B} \mathbf{e}_A \otimes \mathbf{e}_B \otimes \mathbf{e}_C \otimes \mathbf{e}_D. \end{aligned} \quad (44)$$

504 The cell problem for  $\boldsymbol{\omega}$  is given by

$$\left\{ \begin{array}{ll} \text{Div}_Y [\mathcal{C}_R : \text{Grad}_Y \boldsymbol{\omega} - \text{Grad}_Y \boldsymbol{\omega}(\mathcal{C}_R : \mathbf{E}_p^{(0)})] \\ \quad = \text{Div}_Y [\mathcal{C}_R : \mathbf{E}_p^{(0)}], & \text{in } \mathcal{Y}_0 \setminus \Gamma_0 \times \mathcal{T}, \\ \llbracket \boldsymbol{\omega} \rrbracket = \mathbf{0}, & \text{on } \Gamma_0 \times \mathcal{T}, \\ \llbracket (\mathcal{C}_R : \text{Grad}_Y \boldsymbol{\omega} - \text{Grad}_Y \boldsymbol{\omega}(\mathcal{C}_R : \mathbf{E}_p^{(0)}) \\ \quad - \mathcal{C}_R : \mathbf{E}_p^{(0)}) \cdot \mathbf{N}_Y \rrbracket = \mathbf{0}, & \text{on } \Gamma_0 \times \mathcal{T}. \end{array} \right. \quad (45)$$

505 By virtue of the linearization process, we obtain two auxiliary cell problems  
 506 where the macroscopic term  $\text{Grad}_X \mathbf{u}^{(0)}$  is not explicitly present. Indeed, this  
 507 is in general possible only when accounting for the linearized deformations'  
 508 regime, see also [15]. Then, the dependence of the macro-scale variable is  
 509 given through the tensor  $\mathbf{F}_p^{(0)}$ , which describes the plastic-like distortions.  
 510 Moreover, if  $\mathbf{F}_p^{(0)}$  only depends on time, as is the case in [2], the cell problems

511 are also decoupled in the spatial micro- and macro-variables provided that the  
 512 elasticity tensor solely depends on the microscale variable. The cell problems  
 513 are in any case time-dependent, as they encode the evolution of the material  
 514 response and its link with the plastic-like distortions.

515 *Homogenized problem.* From (36) and the (42), the homogenized problem  
 516 rewrites

$$\begin{cases} \text{Div}_X[\hat{\mathcal{C}}_R : \text{Grad}_X \mathbf{u}^{(0)}] = -\text{Div}_X[\hat{\mathbf{D}}_R], & \text{in } \mathcal{B}_h \times \mathcal{T}, \\ (\hat{\mathcal{C}}_R : \text{Grad}_X \mathbf{u}^{(0)}) \cdot \mathbf{N} + \hat{\mathbf{D}}_R \cdot \mathbf{N} = \bar{\mathbf{T}}, & \text{on } \partial_T \mathcal{B}_h \times \mathcal{T}, \\ \mathbf{u}^{(0)} = \bar{\mathbf{u}}, & \text{on } \partial_u \mathcal{B}_h \times \mathcal{T}, \end{cases} \quad (46)$$

517 where

$$\hat{\mathcal{C}}_R = \langle \mathcal{C}_R + \mathcal{C}_R : T\text{Grad}_Y \boldsymbol{\xi} - T\text{Grad}_Y \boldsymbol{\xi}(\mathcal{C}_R : \mathbf{E}_p^{(0)}) - \mathbf{I} \otimes (\mathcal{C}_R : \mathbf{E}_p^{(0)}) \rangle, \quad (47a)$$

$$\hat{\mathbf{D}}_R = \langle \mathcal{C}_R : \text{Grad}_Y \boldsymbol{\omega} - \text{Grad}_Y \boldsymbol{\omega}(\mathcal{C}_R : \mathbf{E}_p^{(0)}) - \mathcal{C}_R : \mathbf{E}_p^{(0)} \rangle. \quad (47b)$$

518 **Remark 3.** *In the absence of distortions, that is for  $\mathbf{F}_p^\varepsilon = \mathbf{I}$ , the cell prob-*  
 519 *lems (43)-(45) reduce to one single cell problem,*

$$\begin{cases} \text{Div}_Y[\mathcal{C} + \mathcal{C} : T\text{Grad}_Y \boldsymbol{\xi}] = \mathbf{0}, & \text{in } \mathcal{Y}_0 \setminus \Gamma_0 \times \mathcal{T}, \\ \llbracket \boldsymbol{\xi} \rrbracket = \mathbf{0}, & \text{on } \Gamma_0 \times \mathcal{T}, \\ \llbracket (\mathcal{C} + \mathcal{C} : T\text{Grad}_Y \boldsymbol{\xi}) \cdot \mathbf{N}_Y \rrbracket = \mathbf{0}, & \text{on } \Gamma_0 \times \mathcal{T}. \end{cases} \quad (48)$$

520 *This is due to the fact that the symmetric tensor  $\mathbf{E}_p^{(0)}$  appearing in (40) is*  
 521 *equal to zero. On the other hand, the homogenized problem is rewritten as*  
 522 *follows,*

$$\begin{cases} \text{Div}_X[\hat{\mathcal{C}} : \text{Grad}_X \mathbf{u}^{(0)}] = \mathbf{0}, & \text{in } \mathcal{B}_h \times \mathcal{T}, \\ (\hat{\mathcal{C}} : \text{Grad}_X \mathbf{u}^{(0)}) \cdot \mathbf{N} = \bar{\mathbf{T}}, & \text{on } \partial_T \mathcal{B}_h \times \mathcal{T}, \\ \mathbf{u}^{(0)} = \bar{\mathbf{u}}, & \text{on } \partial_u \mathcal{B}_h \times \mathcal{T}, \end{cases} \quad (49)$$

523 where  $\hat{\mathcal{C}} = \langle \mathcal{C} + \mathcal{C} : T\text{Grad}_Y \boldsymbol{\xi} \rangle$  is the effective elasticity tensor. Formula-  
 524 tions (48) and (49) are the counterparts of (24) and (25), respectively, when  
 525 plastic-like distortions are neglected and a linearized approach for the defor-  
 526 mations is considered. Particularly, (48) and (49) identify identically with  
 527 classical results in the asymptotic homogenization literature [5, 77].

528 *5.2. Evolution law*

529 Several procedures can be adopted to establish a proper evolution law  
530 for the inelastic distortions. One choice is to follow a phenomenological  
531 approach, which should be based on experimental evidences and comply with  
532 suitable constitutive requirements [29]. On the other hand, one could invoke  
533 some general principles, such as the invariance of the evolution law with  
534 respect to a class of transformations and thermodynamic constraints [21, 22,  
535 23]. Within the latter approach, and adapting the theoretical framework  
536 explored in [21, 22, 23, 29], an evolution equation for the inelastic distortions  
537 has been studied in [19]. Therein, the plastic-like distortions describe a  
538 remodeling process with the following assumptions: (i)  $\mathbf{F}_p$  is restricted by the  
539 constraint  $J_p = 1$ , (ii) the solid phase exhibits hyperelastic behavior, and (iii)  
540 the considered system remodels when the stress induced by external loading  
541 exceeds a characteristic threshold. An evolution law for  $\mathbf{F}_p$  satisfying with  
542 these conditions, and compatible with the Dissipation inequality [12, 32, 33,  
543 34], is given by

$$\text{sym} \left( \mathbf{C} \mathbf{F}_p^{-1} \dot{\mathbf{F}}_p \right) = \gamma \left[ \|\text{dev} \boldsymbol{\sigma}\| - \sqrt{\frac{2}{3}} \sigma_y \right]_+ \frac{\text{dev}(\boldsymbol{\Sigma}) \mathbf{C}}{\|\text{dev} \boldsymbol{\sigma}\|}, \quad (50)$$

544 where  $\boldsymbol{\sigma}$  is the Cauchy stress tensor,  $\text{dev}(\boldsymbol{\Sigma}) = \boldsymbol{\Sigma} - \frac{1}{3} \text{tr}(\boldsymbol{\Sigma}) \mathbf{I}$ , with  $\boldsymbol{\Sigma} = \mathbf{C} \mathbf{S}$   
545 being the Mandel stress tensor, and  $\mathbf{S} = \mathbf{F}^{-1} \mathbf{T}$  the second Piola-Kirchhoff  
546 stress tensor. Moreover,  $\gamma$  is a strictly positive model parameter,  $\sigma_y > 0$   
547 is the yield, or threshold stress, and the operator  $[A]_+$  is such that, for any real  
548 number  $A$ ,  $[A]_+ = A$ , if  $A > 0$ , and  $[A]_+ = 0$  otherwise. [As anticipated in  
549 the Introduction, in the present context the physical meaning of the plastic-  
550 like distortions, represented by  \$\mathbf{F}\_p\$ , is that of structural reorganization, i.e.  
551 remodeling, as is the case in biological tissues when the adhesion bonds  
552 among cells or the structure of the ECM reorganize themselves.](#)

553 Although Equation (50) has been successfully used to describe some bi-  
554 ological situations in which the onset of remodeling is subordinated to the  
555 excess of the yield stress  $\sigma_y$ , the homogenization of the evolution law (50) is  
556 too complicated. For this reason, in this work, we replace (50) with a much  
557 easier law of the type

$$\text{sym} \left( \mathbf{C} (\mathbf{F}_p)^{-1} \dot{\mathbf{F}}_p \right) = \gamma \text{dev}(\boldsymbol{\Sigma}) \mathbf{C}, \quad (51)$$

558 according to which no stress-activation criterion is supplied. Clearly, this  
559 choice may turn out to be unrealistic in many circumstances, but it can

560 still be useful to understand the essence of some stress-driven remodeling  
 561 processes.

562 We need to clarify that, although in some sentences of this work we  
 563 mentioned growth, our model focuses on *pure* remodeling. This is reflected  
 564 by the condition  $\det \mathbf{F}_p = 1$ , and, more importantly, by the fact that the  
 565 evolution laws (50)–(52) are triggered and controlled exclusively by mechan-  
 566 ical factors. On the one hand, the requirement  $\det \mathbf{F}_p = 1$  means that the  
 567 plastic-like distortions are isochoric and, thus, unable to describe volumetric  
 568 growth. On the other hand, the evolution laws for  $\mathbf{F}_p$ , i.e., Equations (50)–  
 569 (52), imply that remodeling is viewed as a consequence of the mechanical  
 570 environment only: When mechanical stress exceeds a given threshold (see  
 571 also [29, 34]), the internal structure of the tissue starts to vary. In other  
 572 words, in the present framework, no biochemical phenomena are accounted  
 573 for as possible activators of remodeling. This is a remarkable difference with  
 574 growth, which, in contrast, occurs only when the concentration of nutrients  
 575 is above a certain threshold value [2, 10, 3, 26, 52]. Our results do not apply  
 576 to growth as they stand, nonetheless, the theory can be adapted to model  
 577 growth by doing some necessary modifications. This is the reason why in  
 578 the abstract we stated that our study offers “*a robust framework that can be*  
 579 *readily generalized to growth and remodeling of nonlinear composites*”.

580 To homogenize (51), the first step is to rewrite it as

$$\text{sym} \left( \mathbf{C}^\varepsilon (\mathbf{F}_p^\varepsilon)^{-1} \dot{\mathbf{F}}_p^\varepsilon \right) = \gamma^\varepsilon \text{dev}(\boldsymbol{\Sigma}^\varepsilon) \mathbf{C}^\varepsilon, \quad (52)$$

581 by admitting that  $\gamma^\varepsilon(X) = \gamma(X, Y)$  is a rapidly oscillating strictly positive  
 582 function. Moreover, by performing the power expansion for  $\boldsymbol{\Sigma}^\varepsilon$ ,

$$\boldsymbol{\Sigma}^\varepsilon(X, t) = \sum_{k=0}^{+\infty} \boldsymbol{\Sigma}^{(k)}(X, Y, t) \varepsilon^k, \quad (53)$$

583 and using (31), the leading order term of  $\boldsymbol{\Sigma}^\varepsilon$  is

$$\boldsymbol{\Sigma}^{(0)} = \mathbf{C}^{(0)} [\mathcal{C}_R : (\mathbf{E}^{(0)} - \mathbf{E}_p^{(0)})]. \quad (54)$$

584 In the limit of small elastic deformations, in (54) we must neglect non-linear  
 585 terms in  $\mathbf{H}$ . Therefore,  $\boldsymbol{\Sigma}^{(0)}$  is approximated with

$$\boldsymbol{\Sigma}_{\text{lin}}^{(0)} = \mathcal{C}_R : \text{sym} \mathbf{H} - (\mathbf{I} + 2 \text{sym} \mathbf{H}) (\mathcal{C}_R : \mathbf{E}_p^{(0)}).$$

586 By virtue of (12a),  $\text{sym}\mathbf{H}$  splits additively as the sum of

$$\text{sym}\mathbf{H} = \mathbf{E}_X^{(0)} + \mathbf{E}_Y^{(1)}, \quad (55)$$

587 where, for  $k = 0, 1$ , and  $j_k = X, Y$ ,

$$\mathbf{E}_j^{(k)} = \frac{1}{2} [\text{Grad}_j \mathbf{u}^{(k)} + (\text{Grad}_j \mathbf{u}^{(k)})^T]. \quad (56)$$

588 By using (55) and (42), we can now rewrite  $\Sigma_{\text{lin}}^{(0)}$  as

$$\Sigma_{\text{lin}}^{(0)} = \mathcal{A}_R : \text{Grad}_X \mathbf{u}^{(0)} + \mathcal{B}_R : \text{Grad}_Y \boldsymbol{\omega} - \mathcal{C}_R : \mathbf{E}_p^{(0)}, \quad (57)$$

589 with

$$\begin{aligned} \mathcal{A}_R &= \mathcal{C}_R + \mathcal{C}_R : T\text{Grad}_Y \boldsymbol{\xi} - \mathbf{I} \underline{\otimes} (\mathcal{C}_R : \mathbf{E}_p^{(0)}) \\ &\quad + [\mathbf{I} \underline{\otimes} (\mathcal{C}_R : \mathbf{E}_p^{(0)})] : [T\text{Grad}_Y \boldsymbol{\xi} + {}^t(T\text{Grad}_Y \boldsymbol{\xi})], \end{aligned} \quad (58a)$$

$$\mathcal{B}_R = \mathcal{C}_R + \mathbf{I} \underline{\otimes} (\mathcal{C}_R : \mathbf{E}_p^{(0)}). \quad (58b)$$

590 In Equation (58a), the symbol  ${}^t(\bullet)$  transposes the fourth-order tensor to  
 591 which it is applied by exchanging the order of its first pair of indices only,  
 592 i.e., given an arbitrary fourth-order tensor  $\mathcal{T} = \mathcal{T}_{ABCD} \mathbf{e}_A \otimes \mathbf{e}_B \otimes \mathbf{e}_C \otimes \mathbf{e}_D$ ,  
 593  ${}^t\mathcal{T}$  reads

$${}^t\mathcal{T} = \mathcal{T}_{BACD} \mathbf{e}_A \otimes \mathbf{e}_B \otimes \mathbf{e}_C \otimes \mathbf{e}_D. \quad (59)$$

594 Note that in the calculations performed to obtain  $\mathcal{A}_R$  and  $\mathcal{B}_R$  in (57), we  
 595 employed the following properties: given two second-order tensors  $\mathbf{A}$  and  $\mathbf{U}$ ,  
 596 with  $\mathbf{A}$  being symmetric, it holds that

$$\mathbf{U}\mathbf{A} = (\mathbf{I} \underline{\otimes} \mathbf{A}) : \mathbf{U}, \quad (60a)$$

$$\mathbf{U}^T \mathbf{A} = (\overline{\mathbf{I}} \underline{\otimes} \mathbf{A}) : \mathbf{U}. \quad (60b)$$

597 Finally, by substituting the expansions of  $\Sigma^\varepsilon$  and  $\mathbf{F}_p^\varepsilon$  in (52), equating  
 598 the leading order terms, excluding non-linear terms of  $\mathbf{H}$  and averaging, the  
 599 homogenized evolution law for the plastic-like distortions is

$$\text{sym} [\langle \mathbf{C}_{\text{lin}}^{(0)} (\mathbf{F}_p^{(0)})^{-1} \dot{\overline{\mathbf{F}_p^{(0)}}} \rangle] = -\langle \gamma \text{dev}(\Sigma_{\text{lin}}^{(0)}) \rangle - \langle \gamma (\mathcal{C}_R : \mathbf{E}_p^{(0)}) (\mathbf{C}_{\text{lin}}^{(0)} - \mathbf{I}) \rangle, \quad (61)$$

600 where  $\Sigma_{\text{lin}}^{(0)}$  is given in (57) and

$$\mathbf{C}_{\text{lin}}^{(0)} = \mathbf{I} + 2\text{sym}\mathbf{H}$$

$$= \mathbf{I} + 2(\mathcal{I} + \mathcal{I} : T\text{Grad}_Y \boldsymbol{\xi}) : \text{Grad}_X \mathbf{u}^{(0)} + 2\mathcal{I} : \text{Grad}_Y \boldsymbol{\omega}. \quad (62)$$

601 We note that, to compute  $\mathbf{C}_{\text{lin}}^{(0)}$ , we must first determine  $\boldsymbol{\xi}$  and  $\boldsymbol{\omega}$ , which is  
 602 done by solving the local problems (43) and (45). Furthermore, Equation  
 603 (61) needs to be supplemented with an initial condition for  $\mathbf{F}_p^{(0)}$ .

604 **Remark 4.** *In the linearized theory of elasticity, even when the individual*  
 605 *constituents of a given composite material are isotropic, the effective elas-*  
 606 *tic coefficients may turn out to be anisotropic, depending on the geometric*  
 607 *properties of the micro-structure. In fact, when the Homogenization Theory*  
 608 *is applied, the anisotropy arises quite naturally due to the solution of the*  
 609 *local cell problems [5, 8]. In fact, the homogenized material is anisotropic*  
 610 *also in the case of rather simple cells, see for instance [61], where an ex-*  
 611 *PLICIT deviation-from- isotropy function is introduced in the context of cubic*  
 612 *symmetric elasticity tensors arising from asymptotic homogenization. This*  
 613 *has noticeable repercussions also on the evolution law that should be chosen*  
 614 *for a correct description of remodeling. To see this, we first notice that, for*  
 615 *an isotropic medium, the evolution law of the plastic-like distortions can be*  
 616 *formulated in terms of tensor  $\mathbf{B}_p$ , since the constitutive framework is such*  
 617 *that  $\mathbf{F}_p$  does not feature explicitly in any constitutive function (see e.g. [78]).*  
 618 *In such cases, a possible evolution law for  $\mathbf{B}_p$  may be given in the form*

$$\dot{\mathbf{B}}_p = \gamma \mathbf{B}_p \text{dev}(\boldsymbol{\Sigma}). \quad (63)$$

619 Equation (63) is, in fact, in harmony with the symmetry properties of the  
 620 material Mandel stress tensor,  $\boldsymbol{\Sigma}$ , i.e.,  $\mathbf{B}_p \boldsymbol{\Sigma} = (\mathbf{B}_p \boldsymbol{\Sigma})^T$  [54]. However, if  
 621 one writes an equation of the same type as (63) at the scale of a cell problem  
 622 (which seems to be a justified choice, because the material is isotropic at  
 623 that scale), and then homogenizes, one ends up with a material for which  
 624 the Mandel stress tensor  $\boldsymbol{\Sigma}$  no longer obeys the symmetry condition  $\mathbf{B}_p \boldsymbol{\Sigma} =$   
 625  $(\mathbf{B}_p \boldsymbol{\Sigma})^T$ . This is because the material is not isotropic at the macroscale  
 626 and, thus, the description of remodeling based on  $\mathbf{B}_p$  becomes inadequate.  
 627 Therefore, if one wants to homogenize, one should start with evolution laws  
 628 at the microscale, which have to be suitable to account for anisotropy, even  
 629 though the single constituents are isotropic at that scale. These considerations  
 630 lead us to Equation (52), as suggested in [22, 23], and subsequently employed  
 631 in [19].

632 **Remark 5.** Equations (50)–(52) can be obtained by adhering to the philos-  
633 ophy presented in [12, 18], and subsequently adopted, for example, in [3] for  
634 growth, in [44] for growth and remodeling, and in [31, 32] for remodeling  
635 only. Accordingly,  $\mathbf{F}_p$  is regarded as the kinematic descriptor of the struc-  
636 tural degrees of freedom of the medium, and  $\dot{\mathbf{F}}_p$  as the generalized velocity  
637 with which the structural changes occur. Within this setting, it can be proven  
638 that for growth and remodeling problems, the dissipation inequality reads

$$\mathcal{D} = \mathbf{Y}_\nu : \mathbf{L}_p + \mathcal{D}_{\text{nc}} \geq 0, \quad (64)$$

639 where  $\mathcal{D}_{\text{mech}} := \mathbf{Y}_\nu : \mathbf{L}_p$  is the mechanical contribution to dissipation, with  
640  $\mathbf{Y}_\nu$  being the dissipative part of a generalized internal force, dual to  $\mathbf{L}_p$ . In  
641 our work, however,  $\mathbf{Y}_\nu$  can be identified with the tensor  $\mathbf{Y}_\nu \equiv J_p^{-1} \mathbf{F}_p^{-\text{T}} \boldsymbol{\Sigma} \mathbf{F}_p^{\text{T}}$ ,  
642 so that  $\mathcal{D}_{\text{mech}}$  coincides with the mechanical dissipation encountered in the  
643 standard formulation of Elastoplasticity, i.e.,  $\mathcal{D}_{\text{mech}} = J_p^{-1} \mathbf{F}_p^{-\text{T}} \boldsymbol{\Sigma} \mathbf{F}_p^{\text{T}} : \mathbf{L}_p =$   
644  $J_p^{-1} \boldsymbol{\Sigma} : \mathbf{F}_p^{-1} \dot{\mathbf{F}}_p$ .

645 In the terminology of [45, 30],  $\mathcal{D}_{\text{nc}}$  is referred to as “non-compliant”  
646 contribution to the overall dissipation. Physically, it summarizes a class of  
647 phenomena that are not —or cannot be— resolved in terms of mechanical  
648 power at the scale of which the dissipation inequality is written. For instance,  
649 in the case of growth,  $\mathcal{D}_{\text{nc}}$  may represent biochemical effects contributing to  
650 the overall dissipation.

651 The inequality (64) can be studied in several ways, depending on the prob-  
652 lem at hand. First, we consider a growth problem. To this end, we assume  
653 that  $\mathcal{D}_{\text{nc}}$  can be written as  $\mathcal{D}_{\text{nc}} = r\mathcal{A}$ , where  $r$  is the rate at which mass  
654 is added or depleted from the system (its units are given by the reciprocal  
655 of time), and  $\mathcal{A}$  is the energy density (per unit volume) associated with the  
656 introduction or uptake of mass. In this setting, it is possible to conceive a  
657 particular state of the system in which the mechanical stress is null, i.e.,  
658  $\boldsymbol{\Sigma} = \mathbf{0}$ , while  $r$  and  $\mathcal{A}$  are generally nonzero. When this occurs, the system  
659 grows without mechanical dissipation, i.e.,  $\mathcal{D}_{\text{mech}} = 0$ , whereas the overall  
660 dissipation of the system reduces to the non-compliant one:

$$\mathcal{D} \equiv \mathcal{D}_{\text{nc}} = r\mathcal{A} \geq 0. \quad (65)$$

661 The second case addresses the situation of pure remodeling, for which we  
662 set  $\mathcal{D}_{\text{nc}} = 0$ , so that the dissipation inequality (64) becomes

$$\mathcal{D} = \mathcal{D}_{\text{mech}} = \mathbf{Y}_\nu : \mathbf{L}_p = J_p^{-1} \boldsymbol{\Sigma} : \mathbf{F}_p^{-1} \dot{\mathbf{F}}_p \geq 0. \quad (66)$$

663 *It is possible to show that the evolution laws (50)–(52) are in harmony with*  
 664 *(66).*

## 665 **6. A computational scheme for small deformations**

666 The macro-scale model given by the problems (46) and (61), together  
 667 with the auxiliary cell problems (43) and (45), requires dedicated numerical  
 668 schemes which are subject of our current investigations. The main compu-  
 669 tational challenge is due to the fact that the local problems depend on the  
 670 macro-scale in a time-dependent way. Therefore, at each time, there is a dif-  
 671 ferent cell problem at each macroscopic point  $X \in \mathcal{B}_h$ . Moreover, one has to  
 672 transfer the information (represented by the geometry, material coefficients,  
 673 and unknowns of the problem) from the cell problems to the homogenized  
 674 problem in the domain  $\mathcal{B}_h$ , and vice versa.

675 Here, as a first step towards the numerical study of this kind of problems,  
 676 we propose an algorithm adapted from [31] that could be useful in our case. In  
 677 [31] it is introduced a computational algorithm, named Generalised Plasticity  
 678 Algorithm (GPA), to study the mechanical response of a biological tissue  
 679 that undergoes large deformations and remodeling of its internal structure.  
 680 Following [31], the discrete and linearized version of the problem constituted  
 681 by Equations (43), (45), (46) and (61) is formulated in three steps.

682 *First step.* The weak form of the cell problems (43) and (45), and of the  
 683 homogenized problem (46) can be *formally* rewritten as

$$\mathcal{L}_1^w(\boldsymbol{\xi}, \mathbf{F}_p^{(0)}, \tilde{\boldsymbol{\xi}}) = 0, \quad (67a)$$

$$\mathcal{L}_2^w(\boldsymbol{\omega}, \mathbf{F}_p^{(0)}, \tilde{\boldsymbol{\omega}}) = 0, \quad (67b)$$

$$\mathcal{H}_1^w(\mathbf{u}^{(0)}, \mathbf{F}_p^{(0)}, \tilde{\mathbf{u}}^{(0)}) = 0, \quad (67c)$$

684 where  $\tilde{\boldsymbol{\xi}}$ ,  $\tilde{\boldsymbol{\omega}}$  and  $\tilde{\mathbf{u}}^{(0)}$  are test functions defined in certain Sobolev spaces, and  
 685  $\mathcal{L}_1^w$ ,  $\mathcal{L}_2^w$  and  $\mathcal{H}_1^w$  are suitable integral operators. Together with (67a)-(67b),  
 686 we rewrite in operatorial form also the homogenized problem (61) as

$$\mathcal{H}_2(\boldsymbol{\xi}, \boldsymbol{\omega}, \mathbf{u}^{(0)}, \mathbf{F}_p^{(0)}) = \mathbf{0}. \quad (68)$$

687 Note that (68) is not a weak form because the corresponding equation does  
 688 not involved spatial derivatives of  $\mathbf{F}_p^{(0)}$ .

689 *Second step.* We perform a backward Euler method for discretizing the evo-  
690 lution law for  $\mathbf{F}_p^{(0)}$  given by (68), thereby ending up with the following system  
691 of time-discrete equations,

$$\mathcal{L}_{1[n]}^w(\boldsymbol{\xi}_{[n]}, \mathbf{F}_{p[n]}^{(0)}, \tilde{\boldsymbol{\xi}}) = 0, \quad (69a)$$

$$\mathcal{L}_{2[n]}^w(\boldsymbol{\omega}_{[n]}, \mathbf{F}_{p[n]}^{(0)}, \tilde{\boldsymbol{\omega}}) = 0, \quad (69b)$$

$$\mathcal{H}_{1[n]}^w(\mathbf{u}_{[n]}^{(0)}, \mathbf{F}_{p[n]}^{(0)}, \tilde{\mathbf{u}}^{(0)}) = 0, \quad (69c)$$

$$\mathcal{H}_{2[n]}(\boldsymbol{\xi}_{[n]}, \boldsymbol{\omega}_{[n]}, \mathbf{u}_{[n]}^{(0)}, \mathbf{F}_{p[n]}^{(0)}) = \mathbf{0}, \quad (69d)$$

692 where  $n = 1, \dots, N$  enumerates the nodes of a suitable time grid. We notice  
693 that an explicit time discrete method could be also used. However, when  
694 dealing with problems in Elastoplasticity, this election could lead to instabil-  
695 ities in the solution [78].

696 *Third step.* The operators  $\mathcal{L}_{1[n]}^w$ ,  $\mathcal{L}_{2[n]}^w$ ,  $\mathcal{H}_{1[n]}^w$  and  $\mathcal{H}_{2[n]}$ , are linear in  $\boldsymbol{\xi}_{[n]}$ ,  $\boldsymbol{\omega}_{[n]}$   
697 and  $\mathbf{u}_{[n]}^{(0)}$ , respectively, but, they are nonlinear in  $\mathbf{F}_{p[n]}^{(0)}$ . Thus, to search the  
698 solution to (69a)-(69d), we linearize at each time step according to Newton's  
699 method (with a linesearch). Therefore, at the  $k$ th iteration,  $k \in \mathbb{N}$ ,  $k \geq 1$ ,  
700  $\mathbf{F}_{p[n,k]}^{(0)}$  is written as

$$\mathbf{F}_{p[n,k]}^{(0)} = \mathbf{F}_{p[n,k-1]}^{(0)} + \boldsymbol{\Psi}_{[n,k]}, \quad (70)$$

701 where  $\mathbf{F}_{p[n,k-1]}^{(0)}$  is known and  $\boldsymbol{\Psi}_{[n,k]}$  represents the unknown increment. We  
702 introduce the notation

$$\mathcal{L}_{1[n,k-1]}^w(\boldsymbol{\xi}_{[n]}, \tilde{\boldsymbol{\xi}}) = \mathcal{L}_{1[n]}^w(\boldsymbol{\xi}_{[n]}, \mathbf{F}_{p[n,k-1]}^{(0)}, \tilde{\boldsymbol{\xi}}), \quad (71a)$$

$$\mathcal{L}_{2[n,k-1]}^w(\boldsymbol{\omega}_{[n]}, \tilde{\boldsymbol{\omega}}) = \mathcal{L}_{2[n]}^w(\boldsymbol{\omega}_{[n]}, \mathbf{F}_{p[n,k-1]}^{(0)}, \tilde{\boldsymbol{\omega}}), \quad (71b)$$

$$\mathcal{H}_{1[n,k-1]}^w(\mathbf{u}_{[n]}^{(0)}, \tilde{\mathbf{u}}^{(0)}) = \mathcal{H}_{1[n]}^w(\mathbf{u}_{[n]}^{(0)}, \mathbf{F}_{p[n,k-1]}^{(0)}, \tilde{\mathbf{u}}^{(0)}). \quad (71c)$$

703 Now, for each time step, and at the  $k$ th iteration, we solve

$$\mathcal{L}_{1[n,k-1]}^w(\boldsymbol{\xi}_{[n]}, \tilde{\boldsymbol{\xi}}) = \mathbf{0}, \quad (72a)$$

$$\mathcal{L}_{2[n,k-1]}^w(\boldsymbol{\omega}_{[n]}, \tilde{\boldsymbol{\omega}}) = \mathbf{0}, \quad (72b)$$

$$\mathcal{H}_{1[n,k-1]}^w(\mathbf{u}_{[n]}^{(0)}, \tilde{\mathbf{u}}^{(0)}) = \mathbf{0}, \quad (72c)$$

704 and obtain the “temporary” solutions  $\boldsymbol{\xi}_{[n,k-1]}$ ,  $\boldsymbol{\omega}_{[n,k-1]}$ , and  $\mathbf{u}_{[n,k-1]}^{(0)}$ , respec-  
 705 tively. Then, upon setting

$$\mathcal{H}_{2[n,k-1]} = \mathcal{H}_{2[n]}(\boldsymbol{\xi}_{[n,k-1]}, \boldsymbol{\omega}_{[n,k-1]}, \mathbf{u}_{[n,k-1]}^{(0)}, \mathbf{F}_{p[n,k-1]}^{(0)}), \quad (73a)$$

$$\mathcal{H}_{[n,k-1]} = \mathcal{H}_{[n]}(\boldsymbol{\xi}_{[n,k-1]}, \boldsymbol{\omega}_{[n,k-1]}, \mathbf{u}_{[n,k-1]}^{(0)}, \mathbf{F}_{p[n,k-1]}^{(0)}), \quad (73b)$$

706 we linearize (69d), i.e.,

$$\mathcal{H}_{2[n,k-1]} + \mathcal{H}_{[n,k-1]} : \boldsymbol{\Psi}_{[n,k]} = \mathbf{0}, \quad (74)$$

707 where  $\mathcal{H}_{[n,k-1]}$  is a fourth-order tensor given by the Gâteaux derivative  
 708 of  $\mathcal{H}_{2[n]}$ , computed with respect to its fourth argument, and evaluated in  
 709  $\mathbf{F}_{p[n,k-1]}^{(0)}$ .

710 If the residuum  $\mathbf{F}_{p[n,k]}^{(0)}$  for  $k$  greater than, or equal to, a certain  $k_*$  is less  
 711 than a tolerance  $\delta > 0$ , then we set  $\mathbf{F}_{p[n]}^{(0)} \equiv \mathbf{F}_{p[n,k_*]}^{(0)} = \mathbf{F}_{p[n,k_*-1]}^{(0)} + \boldsymbol{\Psi}_{[n,k_*]}$  and  
 712 we regard it as the solution of Newton’s method. Thus, we compute  $\boldsymbol{\xi}_{[n]}$ ,  $\boldsymbol{\omega}_{[n]}$   
 713 and  $\mathbf{u}_{[n]}^{(0)}$ .

714 These three steps are summarized in the algorithm 1.

---

### Algorithm 1

---

```

1: procedure
2:   for  $n = 1, \dots, N$  do
3:     State  $k = 1$ 
4:     while  $e > \delta$  do (Known  $\mathbf{F}_{p[n,k-1]}^{(0)}$ )
5:       Solve  $\mathcal{L}_{1[n,k-1]}^w$  and  $\mathcal{L}_{2[n,k-1]}^w$  (To find  $\boldsymbol{\xi}_{[n,k-1]}$  and  $\boldsymbol{\omega}_{[n,k-1]}$ )
6:       Solve  $\mathcal{H}_{1[n,k-1]}^w$  (To find  $\mathbf{u}_{[n,k-1]}^{(0)}$ )
7:       Solve  $\mathcal{H}_{1[n,k-1]}^w$  (To find  $\boldsymbol{\Psi}_{[n,k]}$ )
8:        $\mathbf{F}_{p[n,k-1]}^{(0)} \leftarrow \mathbf{F}_{p[n,k-1]}^{(0)} + \boldsymbol{\Psi}_{[n,k]}$ 
9:       Compute  $e$ 
10:       $k = k + 1$ 
11:    end while
12:     $\mathbf{F}_{p[n]}^{(0)} = \mathbf{F}_{p[n,k-1]}^{(0)} + \boldsymbol{\Psi}_{[n,k]}$ 
13:    Solve  $\mathcal{L}_{1[n]}^w$  and  $\mathcal{L}_{2[n]}^w$  (To find  $\boldsymbol{\xi}_{[n]}$  and  $\boldsymbol{\omega}_{[n]}$ )
14:    Solve  $\mathcal{H}_{1[n]}^w$  (To find  $\mathbf{u}_{[n]}^{(0)}$ )
15:    Update micro and macro geometries
16:  end for
17: end procedure

```

---

## 715 7. Numerical results

716 In this section, the potentiality of our model, which is given by Equations  
 717 (43), (45), (46) and (61), is shown by performing numerical simulations. In

718 particular, we make the following considerations.

719 **(i) Geometry.** We consider the composite body  $\mathcal{B}^\varepsilon$  to have a layered three-  
 720 dimensional structure, and we assume that the layers are orthogonal to the  
 721 direction  $\mathcal{E}_3$ , where  $\{\mathcal{E}_A\}_{A=1}^3$  is an orthonormal basis of a system of Cartesian  
 722 coordinates  $\{X_A\}_{A=1}^3$ . In this particular case, the material properties of the  
 723 heterogeneous body only change along the  $\mathcal{E}_3$  direction and thus, they depend  
 724 solely on the coordinate  $X_3$ . Consequently, the benchmark test at hand, can  
 725 be recast into a one dimensional problem, that is, the reference configuration  
 726 of the periodic cell and the body are considered to be the unidimensional  
 727 domains  $\mathcal{Y}_0 = [0, \ell]$  and  $\mathcal{B}_h = [0, L]$ , respectively. We denote with  $\ell$  and  
 728  $L$ , respectively, the dimension of the periodic cell and the body along the  
 729 direction  $\mathcal{E}_3$ . Moreover, we suppose that the interface  $\Gamma_0$  is the middle point  
 730  $\ell/2$ , so that, each material under consideration has the same volume in the  
 731 microscopic cell  $\mathcal{Y}_0$ .

732 **(ii) Material properties.** We prescribe the elasticity tensor  $\mathcal{C}^\varepsilon$  to be in-  
 733 dependent on the macroscale variable  $X_3$ , i.e.  $\mathcal{C}^\varepsilon(X_3) = \mathcal{C}(X_3, Y_3) \equiv \mathcal{C}(Y_3)$ ,  
 734 being  $\{Y_A\}_{A=1}^3$  a system of microscale Cartesian coordinates. In addition, as  
 735 stated above, we consider that the constituents of the heterogeneous mate-  
 736 rial are isotropic, which implies that the non zero components of the  $6 \times 6$   
 737 symmetric matrix representation of  $\mathcal{C}$  are given by

$$[\mathcal{C}]_{11} = [\mathcal{C}]_{22} = [\mathcal{C}]_{33} = \lambda + 2\mu, \quad (75a)$$

$$[\mathcal{C}]_{12} = [\mathcal{C}]_{13} = [\mathcal{C}]_{23} = \lambda, \quad (75b)$$

$$[\mathcal{C}]_{44} = [\mathcal{C}]_{55} = [\mathcal{C}]_{66} = \frac{1}{2}([\mathcal{C}]_{11} - [\mathcal{C}]_{12}) = \mu, \quad (75c)$$

738 where  $\lambda$  and  $\mu$  are Lamé's parameters. We suppose that  $\mathcal{C}$  is piece-wise  
 739 constant, which means that  $\lambda$  and  $\mu$  are defined as

$$\lambda(Y_3) = \begin{cases} \lambda_1, & \text{in } \mathcal{Y}_0^1 \\ \lambda_2, & \text{in } \mathcal{Y}_0^2 \end{cases} \quad \text{and} \quad \mu(Y_3) = \begin{cases} \mu_1, & \text{in } \mathcal{Y}_0^1 \\ \mu_2, & \text{in } \mathcal{Y}_0^2 \end{cases}. \quad (76)$$

740 Furthermore, we consider that  $\gamma$  has the same value in both constituents,  
 741 this means that, it is set already averaged.

742 **(iii) Plastic-like distortions.** We assume that the matrix representa-  
 743 tion of the tensor  $\mathbf{F}_p^{(0)}$  is diagonal with non-zero components  $[\mathbf{F}_p^{(0)}]_{11} = \frac{1}{\sqrt{p}}$ ,

744  $[\mathbf{F}_p^{(0)}]_{22} = \frac{1}{\sqrt{p}}$  and  $[\mathbf{F}_p^{(0)}]_{33} = p$ , where  $p$  is defined as the remodeling pa-  
 745 rameter. Furthermore, we restrict our investigation to the simpler case of  
 746  $\mathbf{F}_p^{(0)}$  depending solely on  $X_3$ . This means that, the plastic-like distortions of  
 747 order  $\varepsilon^0$  are, in a sense, already averaged, and thus variable from one cell  
 748 to the other, not inside them. In other words, we are interested in the pro-  
 749 duction of distortions in the tissue starting from the cell scale, rather than  
 750 from the cell's microstructure. This, of course, does not mean that the cell's  
 751 microstructure does not change.

752 Together with assumption (ii), we find that the  $6 \times 6$  matrix representa-  
 753 tion of the elasticity tensor, pulled-backed to the reference configuration, is  
 754 symmetric, and its non-zero components are given by

$$[\mathcal{C}_R]_{11} = [\mathcal{C}_R]_{22} = (\lambda + 2\mu)p^2, \quad [\mathcal{C}_R]_{33} = (\lambda + 2\mu)p^{-4}, \quad (77a)$$

$$[\mathcal{C}_R]_{12} = \lambda p^2, \quad [\mathcal{C}_R]_{44} = [\mathcal{C}_R]_{55} = \mu p^{-1}, \quad (77b)$$

$$[\mathcal{C}_R]_{13} = [\mathcal{C}_R]_{23} = \lambda p^{-1}, \quad [\mathcal{C}_R]_{66} = \mu p^2. \quad (77c)$$

755 We remark that  $\mathcal{C}_R$  depends on  $X_3$  and time through  $p$ , whereas it inherits  
 756 the dependence of  $\mathcal{C}$  on the micro-scale variable,  $Y_3$ .

757 **(iv) Initial and boundary conditions.** In the present context, we im-  
 758 pose Dirichlet conditions for  $\mathbf{u}^{(0)}$  on the whole boundary  $\partial\mathcal{B}_h$ , i.e. we do not  
 759 consider a Neumann condition and therefore,  $\partial_u\mathcal{B}_h \equiv \partial\mathcal{B}_h$ . We note that,  
 760 although the homogenization process was developed for mixed boundary con-  
 761 ditions, the whole procedure stands, since the type of boundary conditions  
 762 does not play a role in the derivation of the homogenized model. In par-  
 763 ticular, we set  $[\mathbf{u}^{(0)}]_3 = 0$  at  $X_3 = 0$ , and  $[\mathbf{u}^{(0)}]_3 = \frac{u_L t}{t_f}$  at  $X_3 = L$ , where  
 764  $u_L$  is a target value for the displacement in the direction  $\mathcal{E}_3$ . Moreover,  
 765 we enforce an initial spatial distribution for the remodeling parameter  $p$  as  
 766  $p_{\text{in}}(X_3) = \alpha + \beta \cos(\frac{\pi}{L}X_3)$ , where  $\alpha$  and  $\beta$  are constants.

### 767 7.1. Discussion of the numerical results

768 Given the above considerations, we solve the following homogenized equa-  
 769 tions for  $\mathbf{u}^{(0)}$  and  $p$ ,

$$-\frac{\partial}{\partial X_3}([\hat{\mathcal{C}}_R]_{i3n3} \frac{\partial[\mathbf{u}^{(0)}]_n}{\partial X_3}) = \frac{\partial[\hat{\mathbf{D}}_R]_{i3}}{\partial X_3}, \quad \text{for } i = 1, 2, 3 \quad (78a)$$

$$\langle [\mathbf{C}_{\text{lin}}^{(0)}]_{33} \rangle \frac{\partial p}{\partial t} = \frac{\gamma}{3} \langle \text{dev}(\boldsymbol{\Sigma}_{\text{lin}}^{(0)}) \rangle p - \gamma \langle [\mathcal{C}_R]_{33nn} [\mathbf{E}_p]_{nn} ([\mathbf{C}_{\text{lin}}^{(0)}]_{33} - 1) \rangle p, \quad (78b)$$

770 The coefficients  $[\hat{\mathcal{C}}_R]_{ijkl}$ ,  $[\hat{\mathbf{D}}_R]_{ij}$  and  $[\mathbf{C}_{\text{lin}}^{(0)}]_{ij}$  are given by Equations (47a),  
 771 (47b) and (57), respectively, and are to be found by solving the auxiliary cell  
 772 problems for  $\boldsymbol{\xi}$  and  $\boldsymbol{\omega}$ , given by

$$-\frac{\partial}{\partial Y_3}([\mathcal{Q}]_{i3i3} \frac{\partial[\boldsymbol{\xi}]_{ik3}}{\partial Y_3}) = \frac{\partial[\mathcal{Q}]_{i3i3}}{\partial Y_3} \delta_{ik}, \quad \text{for } i, k = 1, 2, 3 \quad (79a)$$

$$-\frac{\partial}{\partial Y_3}([\mathcal{Q}]_{i3i3} \frac{\partial[\boldsymbol{\omega}]_i}{\partial Y_3}) = -\frac{\partial[\mathbf{Q}]_{33}}{\partial Y_3} \delta_{i3}, \quad \text{for } i = 1, 2, 3 \quad (79b)$$

773 with

$$[\mathcal{Q}]_{i3i3} = [\mathcal{C}_R]_{i3i3} - [\mathbf{Q}]_{33}, \quad \text{with } [\mathbf{Q}]_{33} = [\mathcal{C}_R]_{33nn}[\mathbf{E}_p]_{nn}. \quad (80a)$$

774 In this work, we are not interested to address a real world situation. Our  
 775 aim is, instead, to show how the present theoretical framework can be numerically  
 776 simulated. For this reason, the parameters used in our computations  
 777 are arbitrarily chosen (see Table 1).

Parameter	Unit	Value	Parameter	Unit	Value
$L$	[cm]	28.000	$\lambda_1$	[Pa]	1.00
$u_L$	[cm]	1.0000	$\lambda_2$	[Pa]	2.00
$\gamma$	[1/s]	1.0000	$\mu_1$	[Pa]	0.10
$\alpha$	[—]	1.0035	$\mu_2$	[Pa]	0.06
$\beta$	[—]	-0.0035	$t_0$	[s]	0.00
$N$	[—]	4.0000	$t_f$	[s]	10.0

Table 1: Parameters used in the numerical simulations.

778 In Fig. 2, it is plotted the time evolution of the remodeling parameter  
 779  $p$  at two different points of the macroscopic domain, that is at  $X_3 = 7$  cm  
 780 and  $X_3 = 21$  cm. We observe that the evolution of  $p$  is quite different at  
 781 these two points. Indeed, at  $X_3 = 21$  cm,  $p$  increases and it is always greater  
 782 than one. On the contrary, at  $X_3 = 7$  cm, it is monotonically decreasing  
 783 and tends to be lower than one. In Fig. 3, we show the spatial profile of the  
 784 effective coefficients  $[\hat{\mathcal{C}}]_{33}$ ,  $[\hat{\mathcal{C}}_R]_{33}$  and  $[\hat{\mathbf{D}}_R]_{33}$ . The effective coefficient  $[\hat{\mathcal{C}}]_{33}$   
 785 (see Remark 3) can be computed by using the analytical formula (see e.g.  
 786 [56, 69]),

$$\begin{aligned} [\hat{\mathcal{C}}]_{ijkl} = & \langle [\mathcal{C}]_{ijkl} - [\mathcal{C}]_{ijp3}([\mathcal{C}]_{p3s3})^{-1}[\mathcal{C}]_{s3kl} \rangle \\ & + \langle [\mathcal{C}]_{ijp3}([\mathcal{C}]_{p3s3})^{-1} \rangle \langle ([\mathcal{C}]_{s3t3})^{-1} \rangle^{-1} \langle ([\mathcal{C}]_{t3m3})^{-1}[\mathcal{C}]_{m3kl} \rangle. \end{aligned} \quad (81)$$

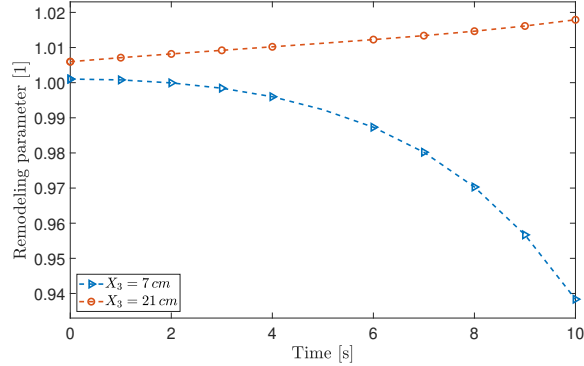


Figure 2: Evolution of the remodeling parameter  $p$  at two different points ( $X_3 = 7$  cm and  $X_3 = 21$  cm) of the macroscopic domain.

787 We observe that even if a loading ramp condition has been imposed on  $\mathbf{u}^{(0)}$   
 788 at the border  $X_3 = L$ , the effective coefficient  $[\hat{\mathcal{E}}]_{33}$  does not vary on time.  
 789 This is because, in contrast to the case in which the plastic-like distortions  
 790 are accounted for, the cell and homogenized problems (cf. (48) and (49)) are  
 791 decoupled. On the other hand, the pulled-back effective coefficients  $[\hat{\mathcal{E}}_{\text{R}}]_{33}$   
 792 and  $[\hat{\mathbf{D}}_{\text{R}}]_{33}$ , given by Equations (47a) and (47b), respectively, do change in  
 793 time since their equations are coupled with an evolution one and, as it can  
 794 be observed, they are strongly influenced by the initial distribution of  $p$ . In  
 795 fact, at the spatial point  $X_3 = 21$  cm, that is, when  $p > 1$ ,  $[\hat{\mathcal{E}}_{\text{R}}]_{33}$  decreases  
 796 and  $[\hat{\mathbf{D}}_{\text{R}}]_{33}$  increases with time. The contrary occurs at  $X_3 = 7$  cm, i.e. when  
 797  $p < 1$ .

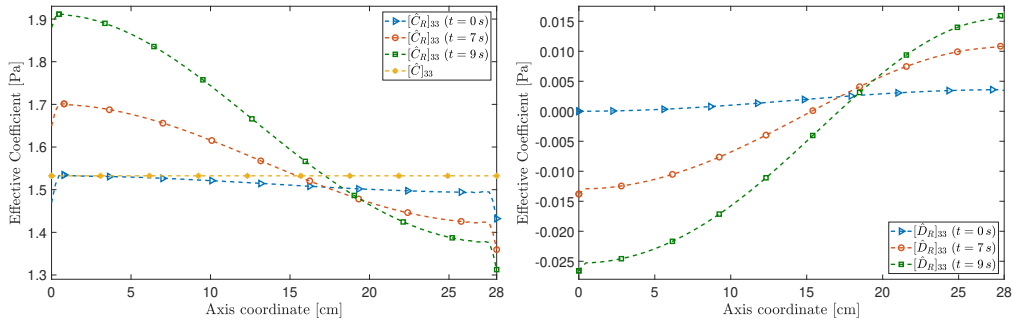


Figure 3: Spatial distribution of the effective coefficients  $[\hat{\mathcal{E}}]_{33}$ ,  $[\hat{\mathcal{E}}_{\text{R}}]_{33}$  and  $[\hat{\mathbf{D}}_{\text{R}}]_{33}$  at different time instants.

798 Additionally, in Fig. 4 it is illustrated the third component of the macro-

799 scopic leading order term of the displacement  $\mathbf{u}^\varepsilon$  at three different time  
800 instants. Particularly, we plot the numerical solution of the homogenized  
801 problems (46) and (49), represented with  $[\mathbf{u}_R^{(0)}]_3$  and  $[\mathbf{u}^{(0)}]_3$ , respectively. We  
802 note that, as expected from our election of the boundary condition, the dis-  
803 placement component augments monotonically in time. However, we notice  
804 that the introduction of the plastic-like distortions, has a direct impact on  
805 the displacement distribution in the interior macroscopic points. Specifically,  
806 in these points the displacement has a higher magnitude.

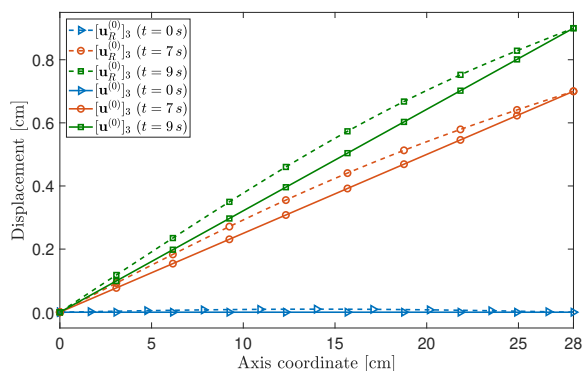


Figure 4: Spatial distribution of the macroscopic leading order term of the displacement with remodeling ( $[\mathbf{u}_R^{(0)}]_3$ ) and without remodeling ( $[\mathbf{u}^{(0)}]_3$ ).

807 The situation described in our numerical simulations, although simplified,  
808 could be a good starting point in the study of the remodeling of biological  
809 tissues. For example, the geometrical properties of bone's osteons permit to  
810 model them as layered composites (see e.g. [69]).

## 811 8. Concluding remarks

812 In the present work, we studied the dynamics of a heterogeneous material,  
813 constituted by two hyperelastic media, with evolving micro-structure by the  
814 application of the asymptotic homogenization technique. The evolution of  
815 the micro-structure of the composite media was characterized through the  
816 development of plastic-like distortions, which were described by means of the  
817 BKL decomposition.

818 The asymptotic homogenization method was applied to a set of problems  
819 comprising a scale-dependent, quasi-static law of balance of linear momen-  
820 tum and an evolution law for the tensor of plastic-like distortions. After

821 obtaining the local and homogenized problems, we rewrote them by consid-  
822 ering the De Saint-Venant strain energy density within the limit of small  
823 deformations. Although the selection of the strain energy density was due  
824 to its simplicity, it is helpful for the description of remodeling processes un-  
825 dergoing small deformations. For instance, this could be the case for the  
826 modeling bone aging. Then, the theoretical setting developed in the present  
827 work is applicable (Elastoplasticity is actually quite appropriate to model  
828 the bone [73]). In such a case, appropriate constitutive laws describing the  
829 progression of the material properties should be found based on experimental  
830 literature (e.g. [35]). Nevertheless, for studying a larger range of problems,  
831 we need to select nonlinear constitutive laws and write the corresponding cell  
832 and homogenized problems.

833 As a consequence of the introduction of the tensor of plastic distortions,  
834 two independent cell problems were inferred, which reduce to the classical  
835 cell problems encountered through a homogenization process in linear elas-  
836 tostatics. We proposed an evolution equation for the inelastic distortions  
837 describing a remodeling process. Such evolution law models a stress-driven  
838 production of inelastic distortions, as the one that is often encountered in  
839 studies of inelastic processes constructed on the decomposition given by (5)  
840 [78]. Thus, the evolution law is suitable for the case of finite strain Elasto-  
841 plasticity, and for the case of remodeling of biological tissues. Finally, we  
842 outlined a computational procedure in order to solve the up-scaled problems  
843 and perform numerical simulations for a particular case where the composite  
844 body is considered to be a layered one. Besides, we assumed that the leading  
845 order term of the asymptotic expansion of the tensor of plastic distortions  
846  $\mathbf{F}_p^{(0)}$  was considered to depend only on the macro-scale variable  $X$ . This  
847 consideration, however, might be relaxed by allowing  $\mathbf{F}_p^{(0)}$  to take into ac-  
848 count the heterogeneities of the composite material through the microscopic  
849 spatial variable  $Y$ . The numerical results showed the influence of the plastic-  
850 like distortions on both the effective coefficients and the macroscopic leading  
851 order term of the displacement.

852 As future work, we intend to deal with the resolution of a particular  
853 problem, like for instance the modeling of bones [49], tumor growth [67, 2,  
854 43, 52, 70, 71], or tissue aging [20]. A further step could be the study, with  
855 the aid of the Homogenization Theory, of the coupling between the results  
856 presented in this work and the fluid flow in a hydrated tissue, or in the case  
857 of wavy laminar structures.

858 **Acknowledgments**

859 AR is financially supported by INdAM. RR gratefully acknowledges the  
860 “Proyecto Nacional de Ciencias Básicas”, Cuba 2015-2018. JM and RP ac-  
861 knowledge support from the Ministry of Economy in Spain (project reference  
862 DPI2014-58885-R).

863 **Declaration of interest**

864 The Authors declare that they have no conflict of interest.

865 **Bibliography**

- 866 [1] Allaire, G., Briane, M. (1996). *Multiscale convergence and reiterated*  
867 *homogenisation*. Proceedings of the Royal Society of Edinburgh: Section  
868 A Mathematics 126:297-342.
- 869 [2] Ambrosi, D., Mollica, F. (2002). *On the mechanics of a growing tumor*.  
870 International Journal of Engineering Science 40:1297-1316.
- 871 [3] Ambrosi, D., Guana, F. (2007). *Stress-modulated growth*. Mathematics  
872 and Mechanics of Solids 12:319-342.
- 873 [4] Auriault, J. L., Boutin, C., Geindreau, C. (2009). *Homogenization of*  
874 *Coupled Phenomena in Heterogenous Media*. ISTE, London, UK; J. Wi-  
875 ley, New Jersey, EE. UU.
- 876 [5] Bakhvalov, N., Panasenko, G. (1989). *Homogenization: Averaging pro-*  
877 *cesses in periodic media*. Kluwer, Dordrecht, The Netherlands.
- 878 [6] Benveniste, Y. (2006). *A general interface model for a three-dimensional*  
879 *curved thin anisotropic interphase between two anisotropic media*. Jour-  
880 nal of the Mechanics and Physics of Solids, 54(4):708-734.
- 881 [7] Benveniste, Y. and Miloh, T. (2001). *Imperfect soft and stiff interfaces*  
882 *in two-dimensional elasticity*. Mechanics of Materials, 33(6):309-323.
- 883 [8] Bensoussan, A., Lions, J.-L., Papanicolaou, G. (1978). *Asymptotic Anal-*  
884 *ysis for Periodic Structures*. AMS Chelsea Publishing.

- 885 [9] Burridge, R., Keller, J. B. (1981). *Poroelasticity equations derived*  
886 *from microstructure*. The Journal of the Acoustical Society of Amer-  
887 ica 70:1140-1146.
- 888 [10] Byrne, H. (2003). *Modelling avascular tumour growth* in L. Preziosi Ed.  
889 *Cancer modelling and simulations*. Chapman & Hall/CRC.
- 890 [11] Castañeda, P. P. (1991). *The effective mechanical properties of nonlinear*  
891 *isotropic composites*. Journal of the Mechanics and Physics of Solids  
892 39:45-71.
- 893 [12] Cermelli, P., Fried, E., Sellers, S. (2001). *Configurational stress, yield*  
894 *and flow in rate-independent plasticity*. Proceedings of the Royal Society  
895 A 457:1447-1467.
- 896 [13] Ciarletta, P., Destrade, M., and Gower, A. L. (2016). *On residual*  
897 *stresses and homeostasis: an elastic theory of functional adaptation in*  
898 *living matter*. Scientific Reports, 6(1).
- 899 [14] Cioranescu, D., Donato, P. (1999). *An Introduction to Homogenization*.  
900 Oxford University Press Inc., New York, EE. UU.
- 901 [15] Collis, J., Brown, D. L., Hubbard, M. E., O’Dea, R. D. (2017). *Effective*  
902 *equations governing an active poroelastic medium*. Proceedings of the  
903 Royal Society A 473:20160755.
- 904 [16] Cowin, S. C. (2000). *How is a tissue built?* Journal of Biomechanical  
905 Engineering, 122(6):553.
- 906 [17] Curnier, A., He, Q.-C., Zysset, P. (1995). *Conewise linear elastic mate-*  
907 *rials*. Journal of Elasticity 37:1-38.
- 908 [18] Di Carlo, A., Quiligotti, S. (2002). *Growth and balance*. Mechanics Re-  
909 search Communications 29:449-456.
- 910 [19] Di Stefano, S., Carfagna, M., Knodel, M. M., Hashlamoun, K., Federico  
911 S., Grillo A. *Anelastic reorganisation in fibre-reinforced biological tissues*.  
912 Submitted.
- 913 [20] Epstein, M. (2009). *The split between remodelling and aging*. Interna-  
914 tional Journal of Non-Linear Mechanics 44.

- 915 [21] Epstein, M., Elżanowski, M. (2007). *Material inhomogeneities and their*  
916 *evolution. A geometric approach*. Springer-Verlag Berlin Heidelberg.
- 917 [22] Epstein, M., Maugin, G. A. (1996). *On the geometrical material struc-*  
918 *ture of anelasticity*. Acta Mechanica 115.
- 919 [23] Epstein, M., Maugin, G. A. (2000). *Thermomechanics of volumetric*  
920 *growth in uniform bodies*. International Journal of Plasticity 16:951-978.
- 921 [24] Fang, Z., Yan, C., Sun, W., Shokoufandeh, A., Regli, W. (2005). *Homog-*  
922 *enization of heterogeneous tissue scaffold: A comparison of mechanics,*  
923 *asymptotic homogenization, and finite element approach*. Applied Bion-
- 924 *ics and Biomechanics 2:17-29.*
- 925 [25] Federico, S. (2012). *Covariant formulation of the tensor algebra of non-*  
926 *linear elasticity*. International Journal of Non-Linear Mechanics 47:273-
- 927 *284.*
- 928 [26] Ganghoffer, J.-F. (2010). *On Eshelby tensors in the context of thermo-*  
929 *dynamics of open systems: Applications to volumetric growth*. Interna-
- 930 *tional Journal of Engineering Science 48:2081-2098.*
- 931 [27] Ganghoffer, J.-F. (2013). *A kinematically and thermodynamically con-*  
932 *sistent volumetric growth model based on the stress-free configuration*.  
933 *International Journal of Solids and Structures 50:3446-3459.*
- 934 [28] Gei, M., Genna, F., Bigoni, D. (2002). *An Interface Model for the Pe-*  
935 *riodontal Ligament*. Journal of Biomechanical Engineering, 124(5):538.
- 936
- 937 [29] Givero, C., Preziosi, L. (2012). *Modelling the compression and reorga-*  
938 *nization of cell aggregates*. Mathematical Medicine and Biology 29:181-
- 939 *204.*
- 940 [30] Goriely, A. (2017). *The Mathematics and Mechanics of Biological*  
941 *Growth*. Springer.
- 942 [31] Grillo, A., Prohl, R., Wittum, G. (2015). *A generalised algorithm for*  
943 *anelastic processes in elastoplasticity and biomechanics*. Mathematics  
944 *and Mechanics of Solids 22:502-527.*

- 945 [32] Grillo, A., Carfagna, M. Federico, S. (2018). *An Allen-Cahn approach*  
946 *to the remodelling of fibre-reinforced anisotropic materials*. Journal of  
947 Engineering Mathematics (In Press).
- 948 [33] Grillo, A., Federico, S., Wittum, G. (2012). *Growth, mass transfer and*  
949 *remodelling in fibre-reinforced multi-constituent materials*. International  
950 Journal of Non-Linear Mechanics 47:388-401.
- 951 [34] Grillo, A., Prohl, R., Wittum, G. (2016). *A poroplastic model of struc-*  
952 *tural reorganisation in porous media of biomechanical interest*. Continuum  
953 Mechanics and Thermodynamics 28:579-601.
- 954 [35] Grynepas, M. (1993). *Age and disease-related changes in the mineral of*  
955 *bone*. Calcified Tissue International 53:57-64.
- 956 [36] Guinovart-Díaz, R., Rodríguez-Ramos, R., Bravo-Castillero, J., López-  
957 Realpozo, J., Sabina, F., Sevostianov, I. (2013). *Effective elastic prop-*  
958 *erties of a periodic fiber reinforced composite with parallelogram-like ar-*  
959 *rangement of fibers and imperfect contact between matrix and fibers*. In-  
960 ternational Journal of Solids and Structures, 50(13):2022-2032.
- 961 [37] Hammer, D. A. and Tirrell, M. (1996). *Biological adhesion at interfaces*.  
962 Annual Review of Materials Science, 26(1):651-691.
- 963 [38] Hashin, Z. (1990). *Thermoelastic properties of fiber composites with im-*  
964 *perfect interface*. Mechanics of Materials, 8(4):333-348.
- 965 [39] Hashin, Z. (2002). *Thin interphase/imperfect interface in elasticity with*  
966 *application to coated fiber composites*. Journal of the Mechanics and  
967 Physics of Solids, 50(12):2509-2537.
- 968 [40] Holmes, M. H. (1995). *Introduction to perturbation methods* (Vol. 20).  
969 Springer Science & Business Media, Springer-Verlag, New York.
- 970 [41] Hori, M., Nemat-Nasser, S. (1999). *On two micromechanics theories for*  
971 *determining micromacro relations in heterogeneous solids*. Mechanics of  
972 Materials 31:667-682.
- 973 [42] Javili, A., Steinmann P., Kuhl, E. (2014). *A novel strategy to identify*  
974 *the critical conditions for growth-induced instabilities*. Journal of the  
975 Mechanical Behavior of Biomedical Materials 29:20-32.

- 976 [43] Jain, R. K., Martin, J. D., Stylianopoulos, T. (2014). *The role of me-*  
977 *chanical forces in tumor growth and therapy*. Annual Review of Biomed-  
978 ical Engineering 16:321-346.
- 979 [44] Olsson, T., Klarbring, A. (2008). *Residual stresses in soft tissue as a*  
980 *consequence of growth and remodeling: application to an arterial geom-*  
981 *etry*. European Journal of Mechanics A/Solids 27:959-974.
- 982 [45] Kuhl, E., Holzapfel, G.A. (2007). *A continuum model for remodeling in*  
983 *living structures*. Journal of Material Science 42:8811–8823.
- 984 [46] Lefik, M., Schrefler, B. (1996). *Fe modelling of a boundary layer cor-*  
985 *rector for composites using the homogenization theory*. Engineering with  
986 Computers 13:31-42.
- 987 [47] Leyrat, A., Duperray, A., Verdier, C. (2003). *Cancer Modelling and*  
988 *Simulation*, chapter *Adhesion Mechanisms in Cancer Metastasis* Ed.  
989 L. Preziosi. Chapman & Hall/CRC Mathematical and Computational  
990 Biology.
- 991 [48] Lin, W. J., Iafrati, M. D., Peattie, R. A., and Dorfmann, L. (2018).  
992 *Growth and remodeling with application to abdominal aortic aneurysms*.  
993 Journal of Engineering Mathematics, 109(1):113-137.
- 994 [49] Lu, Y., Lekszycki, T. (2016). *Modelling of bone fracture healing: in-*  
995 *fluence of gap size and angiogenesis into bioresorbable bone substitute*.  
996 Mathematics and Mechanics of Solids 22:1997-2010.
- 997 [50] Lubliner, J. (2008). *Plasticity Theory (Dover Books on Engineering)*.  
998 Dover Publications.
- 999 [51] Lukkassen, D., Milton, G. W. (2002). *On hierarchical structures and*  
1000 *reiterated homogenization*. Function Spaces, Interpolation Theory and  
1001 Related Topics 355-368.
- 1002 [52] Mascheroni, P., Carfagna, M., Grillo, A., Boso, D. P., Schrefler, B.  
1003 A. (2018). *An avascular tumor growth model based on porous media*  
1004 *mechanics and evolving natural states*. Mathematics and Mechanics of  
1005 Solids DOI: 10.1177/1081286517711217 (In press).

- 1006 [53] Marsden, J. E., Hughes, T. J. R. (1983). *Mathematical Foundations of*  
1007 *Elasticity*. Dover Publications Inc., New York.
- 1008 [54] Maugin, G. A., Epstein, M. (1998). *Geometrical material structure of*  
1009 *elastoplasticity*. International Journal of Plasticity 14:109-115.
- 1010 [55] Mićunović, M. V. (2009). *Thermomechanics of Viscoplasticity - Funda-*  
1011 *mentals and Applications*. Springer, Heidelberg, Germany
- 1012 [56] Milton, G. W. (2002). *The Theory of Composites*. Cambridge University  
1013 Press .
- 1014 [57] Panasenko, G. (2005). *Multi-Scale Modelling for Structures and Com-*  
1015 *posites*. Springer, Berlin.
- 1016 [58] Parnell, W. J., Vu, M. V., Grimal, Q., Naili, S. (2012). *Analytical meth-*  
1017 *ods to determine the effective mesoscopic and macroscopic elastic prop-*  
1018 *erties of cortical bone*. Biomechanics and Modeling in Mechanobiology  
1019 11:883-901.
- 1020 [59] Penta, R., Ambrosi, D. (2014). *Effective governing equations for poroe-*  
1021 *lastic growing media*. Quarterly Journal of Mechanics and Applied Math-  
1022 ematics 67:69-91.
- 1023 [60] Penta, R., Gerisch, A. (2015). *Investigation of the potential of asymptotic*  
1024 *homogenization for elastic composites via a three-dimensional computa-*  
1025 *tional study*. Computing and Visualization in Science 17:185-201.
- 1026 [61] Penta, R., Gerisch, A. (2017). *The asymptotic homogenization elasticity*  
1027 *tensor properties for composites with material discontinuities*. Contin-  
1028 uum Mechanics and Thermodynamics 29:187-206.
- 1029 [62] Penta, R., Gerisch, A. (2018). *An Introduction to Asymptotic homoge-*  
1030 *nization* in Gerisch, A., Penta, R., Lang., J (eds.) *Multiscale models in*  
1031 *Mechano and Tumor Biology*, Lecture Notes in Computational Science  
1032 and Engineering (122), Springer.
- 1033 [63] Penta, R., Merodio, J. (2017). *Homogenized modeling for vascularized*  
1034 *poroelastic materials*. Meccanica 52:3321-3343.

- 1035 [64] Penta, R., Ramírez-Torres, A., Merodio, J., Rodríguez-Ramos, R.  
1036 (2018). *Effective balance equations for elastic composites subject to in-*  
1037 *homogeneous potentials*. Continuum Mechanics and Thermodynamics  
1038 30:145-163.
- 1039 [65] Penta, R., Raum, K., Grimal, Q., Schrof, S., Gerisch, A. (2016). *Can a*  
1040 *continuous mineral foam explain the stiffening of aged bone tissue? A*  
1041 *micromechanical approach to mineral fusion in musculoskeletal tissues*.  
1042 *Bioinspiration & Biomimetics* 11:035004.
- 1043 [66] Persson, L. E., Persson, L., Svanstedt, N., Wyller, J. (1993). *The ho-*  
1044 *mogenization method. An introduction*. Studentlitteratur, Lund.
- 1045 [67] Preziosi, L., Vitale, G. (2011). *A multiphase model of tumor and tissue*  
1046 *growth including cell adhesion and plastic reorganization*. Mathematical  
1047 Models and Methods in Applied Sciences 21:1901-1932.
- 1048 [68] Pruchnicki, E. (1998). *Hyperelastic homogenized law for reinforced elas-*  
1049 *tomer at finite strain with edge effects*. Acta Mechanica 129:139-162.
- 1050 [69] Ramírez-Torres, A., Penta, R., Rodríguez-Ramos, R., Merodio, J.,  
1051 Sabina, F. J., Bravo-Castillero, J., Guinovart-Díaz, R., Preziosi, L.,  
1052 Grillo, A. (2018). *Three scales asymptotic homogenization and its ap-*  
1053 *plication to layered hierarchical hard tissues*. International Journal of  
1054 Solids and Structures 130-131:190-198.
- 1055 [70] Ramírez-Torres, A., Rodríguez-Ramos, R., Merodio, J., Bravo-  
1056 Castillero, J., Guinovart-Díaz, R., Alfonso, J. C. L. (2015). *Action of*  
1057 *body forces in tumor growth*. International Journal of Engineering Sci-  
1058 ence 89:18-34.
- 1059 [71] Ramírez-Torres, A., Rodríguez-Ramos, R., Merodio, J., Bravo-  
1060 Castillero, J., Guinovart-Díaz, R., Alfonso, J. C. L. (2015). *Mathemati-*  
1061 *cal modeling of anisotropic avascular tumor growth*. Mechanics Research  
1062 Communications 69:8-14.
- 1063 [72] Reimer, P., Parizel, P. M., Meaney, J. F. M., Stichnoth, F. A., editors  
1064 (2010). *Clinical MR Imaging*. Springer Berlin Heidelberg.
- 1065 [73] Ritchie, R. O., Buehler, M. J., Hansma, P. (2009). *Plasticity and tough-*  
1066 *ness in bone*. Physics Today 62:41-47.

- 1067 [74] Rohan, E., Cimrman, R., Lukeš, V. (2006). *Numerical modelling and*  
1068 *homogenized constitutive law of large deforming fluid saturated hetero-*  
1069 *geneous solids*. Composites and Structures 84:1095-1114.
- 1070 [75] Rohan, E., Lukeš, V. (2010). *Microstructure based two-scale modelling*  
1071 *of soft tissues*. Mathematics and Computers in Simulation 80:1289-1301.  
1072
- 1073 [76] Rodriguez, E. K., Hoger, A., McCulloch, A. D. (1994). *Stress-dependent*  
1074 *finite growth in soft elastic tissues*. Journal of Biomechanics 27:455-467.  
1075
- 1076 [77] Sanchez-Palencia, E. (1980). *Non-homogeneous media and vibration the-*  
1077 *ory*. In: Lecture Notes in Physics, 127. Springer-Verlag, Berlin.
- 1078 [78] Simo, J. C., Hughes, T. J. R. (1988). *Computational Plasticity*. Springer,  
1079 New York.
- 1080 [79] Suquet, P. (1987). *Elements of homogenization for inelastic solid me-*  
1081 *chanics* in *Homogenization techniques for composite media*. Eds. E.  
1082 Sanchez-Palencia and A. Zaoui. Springer-Verlag, Berlin.
- 1083 [80] Taber, L. A. (1995). *Biomechanics of growth, remodeling, and morpho-*  
1084 *genesis*. Applied Mechanics Reviews, 48(8):487.
- 1085 [81] Taffetani, M., de Falco, C., Penta, R., Ambrosi, D., Ciarletta, P. (2014).  
1086 *Biomechanical modelling in nanomedicine: multiscale approaches and*  
1087 *future challenges*. Archive of Applied Mechanics 84:1627-1645.
- 1088 [82] Telega, J. J., Galka, A., Tokarzewski, S. (1999). *Application of the reit-*  
1089 *erated homogenization to determination of effective moduli of a compact*  
1090 *bone*. Journal of Theoretical and Applied Mechanics 37(3):687-706.
- 1091 [83] Tsalis, D., Baxevanis, T., Chatzigeorgiou, G., Charalambakis, N. (2013).  
1092 *Homogenization of elastoplastic composites with generalized periodicity*  
1093 *in the microstructure*. International Journal of Plasticity 51:161-187.
- 1094 [84] Walpole, L. J. (1981). *Elastic behaviour of composites materials: theo-*  
1095 *retical foundations*. Advances in Applied Mechanics 21:169-242.

- 1096 [85] Walpole, L. J. (1984). *Fourth-rank tensors of the thirty two crys-*  
1097 *tal classes: multiplication tables*. Proceedings of the Royal Society A  
1098 391:149-179.